

Table 7. Human PCR Primers and Probes for qRT-PCR in PBMNC and QQMNC

Gene	Forward Primer	Reverse Primer	TaqMan Probe (5'-FAM, 3'-BHQ)
VEGF-A	5'-CCCAGGAGACCT 5'-GGTTGTGT-3'	5'-TGGATCCTGCCCTGT CTCTCT-3'	5'-AGTGGTTGACCTTCC TCCATCCCC-3'
VEGF-B	5'-AGGTGACACATG GCTTTTCAG A-3'	5'-GTTCCCCCACTGGGA TATAGC-3'	5'-TCAGCAGGGTGACTT GCCTCAGA-3'
Ang-1	5'-AAGTACTGGGC CTCCTCTCA-3'	5'-CCATTAAGGCAT AGTGGATCAAGTC-3'	5'-AAAAGAGACAGTTGT TGGCAAGGTAGCAA-3'
Ang-2	5'-GCAGGGAGTGG TGAGACAGTT-3'	5'-TGCAGGTGCTATGGT CTTTAGAAT-3'	5'-ACGGCTCCTCAGAAA TCCAGTGACC-3'
IGF-1	5'-GCCCAAATGCA CTGATGTAAA-3'	5'-AGTGACTTTGCTATGAGTTGGTGAGT-3'	5'-CTCTAAAATCCCTTT CAAGCCACCCAT-3'
Leptin	5'-TCACTAGATGGCGAGCATCCT-3'	5'-CACGCTCAGCTAACTTTTGTGTTT-3'	5'-CCAACATGGTGAACCCCGTCTCTAC-3'
IL-8	5'-TTTGATACTCCAGTCTTGTCTATTG-3'	5'-CAAGTTTCAACCAGCAAGAAATTACT-3'	5'-TTAGAACTATTAACAGCCAAAATCCACA-3'
IL-10	5'-GCCTGACCACGCTTTCTAGCT-3'	5'-CCAAGCCAGAGACAAGATAAATT-3'	5'-TTGAGCTGTTTTCCCTGACCTCCC-3'
IL-1 β	5'-CGGCCACATTTGGTTCTAAGA-3'	5'-AGGGAAGCGGTTGCTCATC-3'	5'-ACCCTCTGCTATTGCTCCACA-3'
TGF- β	5'-CCCTGCCCTACATTTGGA-3'	5'-CCGGTTATGCTGGTTGTACA-3'	5'-TGGACACGCAGTACAGCAAGGTCCT-3'
TNF- α	5'-GAGACCAGGGAGCCTTTGGT-3'	5'-TGTGTCAATTTCTAGGTGAGGTCTTC-3'	5'-CTGGCCAGAATGCTGCAGGACTT-3'
MMP-2	5'-GGTCCCCTGTTCACTCTACTTAGC-3'	5'-CGGCTTGGTTTTCTCCAT-3'	5'-TGTCCCTACCGAGTCTCTTCTCCACTG-3'
MMP-9	5'-CCCGAGTGAGTTGAACCA-3'	5'-AGGGCACTGCAGGATGTCA-3'	5'-TGGACCAAGTGGGCTACGTGACCT-3'
GAPDH	5'-GGTGGTCTCCTCTGACTTCAACA-3'	5'-GTGGTCGTTGAGGGCAATG-3'	5'-ACACCCACTCCTCCACCTTTGACG-3'

Ang indicates angiopoietin; GAPDH, glyceraldehyde-3-phosphate dehydrogenase; IGF, insulin-like growth factor; IL, interleukin; MMP, matrix metalloproteinase; PBMNCs, peripheral blood mononuclear cells; QQMNCs, quality and quantity control culture of mononuclear cells; qRT-PCR, quantitative real-time polymerase chain reaction; TGF, transforming growth factor; TNF, tumor necrosis factor; VEGF, vascular endothelial growth factor.

perfusion imaging (LDPI; Moor Instruments, Axminster, UK) were performed under adequate anesthetization by 1.5% to 2.0% isoflurane (Dainippon Sumitomo Pharma Co., Ltd., Osaka, Japan) to minimize pain to mice by regarding the 3Rs (replacement, reduction, and refinement). After surgery, mice were subcutaneously injected with buprenorphine (Repetan, 0.1 mg/kg body weight; Otsuka Pharmaceutical Co., Ltd., Tokyo, Japan) once a day for 3 days to relieve pain or discomfort. At sacrifice, pentobarbital sodium (Somnopen-tyl, 60 to 70 mg/kg body weight; Kyouritu Seiyaku Co., Ltd., Tokyo, Japan) was intraperitoneally injected.

Making ischemic hindlimb model and cell Tx

Eight- to 10-week-old male BALB/c nu/nu mice (CAnN.Cg-Foxn1^{nu}/CriCrlj; Charles River Laboratories Japan, Inc., Tokyo, Japan) were used, as reported elsewhere.²⁶ The proximal portion of the left femoral artery, including the superficial and the deep branch, was suture-ligated, and the proximal and distal portions of the saphenous artery were occluded with a bipolar forcep electric coagulator (MERA N3-14; SENKO MEDICAL INSTRUMENT mfg. Co., Ltd., Tokyo, Japan). The overlying skin was closed with a 6-0 silk suture. The next day, cells were suspended in IMDM medium and intramuscularly injected into ischemic hindlimbs.

The cell injection sites and the doses for assays were as follows: each one site of anterior tibial muscle (ATM) and gastrocnemius muscle (GCM) for blood flow analysis and histology, that is, hematoxylin and eosin (H&E) staining, Azan staining, and inducible nitric oxide synthase (iNOS)

immunohistochemistry (IHC) (5.0×10^3 cells/20 μ L per site: total 1×10^4 cells/mouse), 2 sites of ATM for qRT-PCR (5.0×10^3 cells/20 μ L per site: total 1×10^4 cells/mouse), or for histological assessment by confocal images (1.0×10^5 cells/20 μ L per site: total 2×10^5 cells/mouse).

Assessment of blood flow

LDPI was used to record serial blood flow measurements for 3 weeks after surgery; these data were analyzed using Moor Idi Main software (Laser Doppler Imager ver 5.2; Moor Instruments). The blood flow in identical toe regions of interest (ROIs) between ischemic and contralateral hindlimbs per mouse was measured by LDPI; the blood-flow ratio of ischemic versus contralateral hindlimb was calculated. Mice with toe necrosis or limb salvage were only involved in the calculation, whereas those with foot necrosis or autoamputation were excluded.

Tissue preparation of histochemical assessment

Three weeks after surgery, 40 μ L of Isolectin B4-FITC (Fluorescein Griffonia Simplicifolia Lectin I, Isolectin B4; Vector Laboratories Inc., Burlingame, CA) was injected into the tail vein using a insulin syringe, and then 20 minutes later, mice were sacrificed under adequate anesthetization. Immediately after sacrifice, mice were perfused with 20 mL of PBS and then with the equivalent volume of 4% paraformaldehyde (PFA)/PBS by cardiac puncture. Subsequently, hindlimbs were resected and incubated in 4% PFA/PBS at 4°C overnight. Thereafter, ATMs, after QQMNCtx and PBMNCtx, were

excised and embedded into paraffin for the tissue sample preparation. Alternatively, the muscles, after QQMNCTx, GmCD34Tx, and eEPCTx, were coated with optimal cutting temperature (O.C.T.) compound (Tissue-Tek; Sakura Finetek Japan Co., Ltd., Tokyo, Japan), immediately frozen in liquid nitrogen, and refrigerated until use at -80°C . Cross-sectional tissue samples with the thickness at 6 to 8 μm for paraffin section or at 10 μm for frozen sections, were sliced from tissue blocks of muscles and then subjected to assessments as described below.

Microvasculature and pericyte recruitment

For alpha-smooth muscle actin (α -SMA) staining, paraffin tissue sections, after deparaffinization or the frozen ones, were washed with PBS, blocked with 10% goat serum for 30 minutes at room temperature (RT), then, incubated with Cy3-conjugated anti- α -SMA Ab (Sigma-Aldrich) and prediluted (1:200 ratio) with 1% BSA/PBS for 2 hours at RT. After washing with PBS, sections were mounted with 1.25% (w/v) DABCO (Sigma-Aldrich)/90% (v/v) glycerol/10% (v/v) PBS, then observed using a fluorescent microscope (Bioevo; Keyence Corporation, Osaka, Japan). The same protocol, without using the Ab, was performed as the negative control. Also, the negative control for Isolectin B4-FITC staining was in advance, prepared from the mice without in vivo injecting Isolectin B4-FITC into the tail vein.

Using software (VH analyzer; Keyence), microvascular densities were evaluated by counting the microvessels stained with Isolectin B4-FITC. Simultaneously, pericyte recruitment to the vasculatures was evaluated by counting the α -SMA-positive microvessels.

Myogenesis and interstitial fibrosis

Centrally nucleated muscle fibers stained with H&E were photographed with an automatic research photomicroscope (AX80; Olympus) and were then counted as regenerating muscle fibers implying fusion of myoblasts²⁷ by VH analyzer (Keyence). Limb interstitial fibrosis detected by Azan staining was morphometrically assessed by the same photomicroscope and software.^{28,29}

Tissue inflammation

Paraffin tissue sections were deparaffinized, autoclaved in citrate buffer at 121°C for 10 minutes to retrieve the target antigen, incubated with the primary Ab of rabbit polyclonal anti-iNOS Ab (Abcam, Cambridge, MA) prediluted with 1% BSA/PBS (1:100 ratio) at 4°C overnight (Table 8). Thereafter, samples were treated with 0.3% H_2O_2 /methanol and Histofine Simple Stain MAX PO (Nichirei Biosciences Inc., Tokyo, Japan) and then dyed with 3,3'-diaminobenzidine, tetrahydrochloride (DAB; Dojindo, Kumamoto, Japan). Furthermore, the samples were

Table 8. Primary and Isotype Antibodies to Detect iNOS for Immunohistochemistry

Antibodies	Company, Catalog No.	Final Dilution Ratio or Concentration
Anti-iNOS antibody	Abcam, #ab15323	1:100 in 1% BSA/PBS
Rabbit immunoglobulin fraction (solid-phase absorbed)	Dako, #X0936	2 $\mu\text{g}/\text{mL}$ in 1% BSA/PBS

iNOS indicates inducible nitric oxide synthase.

stained with hematoxylin, dehydrated, and then mounted with malinol. Frozen tissue sections were also stained with the anti-iNOS Ab in the same way, after similar autoclave and subsequent treatment with 0.5% Triton X-100/PBS. Control samples were prepared under the same procedure, using rabbit immunoglobulin fraction (DAKO, Tokyo, Japan).

Vasculogenesis by transplanted cells

The cross-sections at 10 μm from frozen tissues, after washing with PBS, were microwaved in target retrieval solution (Dako) diluted with distilled water (1:10 ratio) at 98°C for 10 minutes. Then, after treatment with a streptavidin/biotin blocking kit (Vector Laboratories) to block endogenous biotin, sections were incubated with 5% goat serum/1% BSA/PBS for 30 minutes at RT. For the preparation of primary Ab to human CD31, mouse anti-human CD31 Ab and biotinylated goat anti-mouse IgG (Fitzgerald Industries International Inc., Acton, MA) were, respectively, diluted in 1% BSA/PBS (1:8 and 1:48 ratio), that is, adjusted to the concentration of 25 and 60 $\mu\text{g}/\text{mL}$. The prediluted reagents were mixed in the equal volume and reacted at RT for 1 hour. The prereacted reagent was further mixed with mouse serum (2:1 ratio; Rockland Immunochemicals, Inc., Gilbertsville, PA) and incubated at RT for 1 hour. The primary Ab reagent for human CD31 was incubated with the tissue sections at 4°C overnight. Sections were washed with PBS and subsequently incubated with streptavidin and Alexa Fluor 594 conjugate prediluted in 1% BSA/PBS (1:90 ratio) at RT for 1 hour. Tissue sections were washed with PBS and finally mounted with 1 $\mu\text{mol}/\text{L}$ of TOTO-3 iodide (Invitrogen) in 1.25% (w/v) DABCO/90% (v/v) glycerol/10% (v/v) PBS. Tissue sections were observed by a confocal laser-scanning microscope (LSM510META; Carl Zeiss GmbH, Jena, Germany). Mouse anti-human CD31 Ab and reagents are detailed in Table 9. The acquired images at 0.8 μm z interval (11 sliced images by 10 intervals at total 8- μm thickness) were reconstructed three-dimensional (3D) structures using the function of 3D spectrum analysis. Furthermore, to quantify "vasculogenic properties" in their images, the surface of a volume object in the ROI, was visualized, using an Imaris iso-surface function of 4D Image analysis software (Imaris 6.2.0; Carl Zeiss): murine

Table 9. Primary and Secondary Antibodies for Immunohistochemistry to Detect Vascular Structures Formed by Transplanted Human Cells

Antibodies	Company, Catalog No.	Final Dilution Ratio
Mouse anti-human CD31	Dako, #M0823	1:24 in 1% BSA/PBS
Goat anti-mouse IgG (H+L) (biotin)	Fitzgerald, #43C-CB1533	1:144 in 1% BSA/PBS
Purified mouse IgG1, isotype control	Dako Cytomation, #X0931	1:6 in 1% BSA/PBS
Streptavidin, Alexa Fluor 594 conjugate	Molecular Probes, #S-11227	1:90 in 1% BSA/PBS

vessels stained with Isolectin B4-FITC (green) and transplanted cell-derived microvessels stained with Alexa 594-conjugated human specific anti-CD31 Ab (red). The values of microvascular density in 2D image and % volume per image cube in 3D were respectively calculated for the green- or red-colored microvessels.

Murine qRT-PCR of ischemic hindlimb

Mice were sacrificed under adequate anesthetization on day 6 after cell Tx. GCMs of ischemic hindlimbs were harvested for total RNA isolation, mice were perfused with 20 mL of PBS by cardiac puncture to remove circulating blood, and GCMs were resected out and incubated into 1 mL of RNA later at 4°C overnight. After homogenization of GCMs with 1 mL of Trizol (Invitrogen), total RNA was isolated and genomic DNA was digested by DNase I treatment (Invitrogen) at 37°C for 15 minutes. DNase I-treated total RNA was purified by phenol extraction and ethanol precipitation. Two micrograms of purified total RNA was used for cDNA synthesis with the High Capacity cDNA Reverse Transcription kit (Applied Biosystems). cDNA mixture was sequentially diluted by 20- to 160-fold with Mili-Q water (Millipore Corporation, Billerica, MA) after first-strand cDNA synthesis. Using ABI Prism 7700 (Applied Biosystems), TaqMan gene expression assays for diluted cDNA were performed with TaqMan Fast Universal PCR Master Mix (Applied Biosystems), according to the manufacturer's protocol. The amplification of cDNA was as follows: denaturation at 95°C for 3 seconds, annealing/extension at 62°C for 30 seconds, and 40 cycles. The relative mRNA expression was calculated by the $\Delta\Delta C_t$ method with normalization to mouse 18S rRNA. All primers and TaqMan probes used are listed in Table 10.

Statistical Analysis

Prism5 software (GraphPad Software Inc., Cary, NC) was used to conduct all statistical analyses. Wilcoxon's signed-rank test

Table 10. Murine PCR Primers and TaqMan Probes for qRT-PCR

Gene	Catalog No.	Company
MyoD1	Mm01203489_g1	Applied Biosystems
Myogenin	Mm00446195_g1	Applied Biosystems
IGF-1	Mm00439560_m1	Applied Biosystems
IL-1 β	Mm00434228_m1	Applied Biosystems
TGF- β	Mm01227699_m1	Applied Biosystems
18S rRNA	Mm03928990_g1	Applied Biosystems

IGF indicates insulin-like growth factor; IL, interleukin; qRT-PCR, quantitative real-time polymerase chain reaction; TGF, transforming growth factor.

or linear regression analysis was used to analyze quantitative variation or correlation of cells and EPC-CFUs between PBMNCs and QQMNCs in each individual. To assess the variation of each hematopoietic cell or helper T subset through QQ culture, Wilcoxon's signed-rank test was also applied for comparison of the ratio of % cell positivity in the whole cells or CD4⁺ T cells of QQMNCs to that of PBMNCs in each individual. Mann-Whitney's U test and Kruskal-Wallis' test were applied to compare the data between 2 groups and among 3 to 4 groups. The experiment to assess angiogenic properties by transplanted human cells using a confocal fluorescence microscope was performed simultaneously on the whole groups: IMDM control, PBMNCTx, eEPCTx, QQMNCTx, and GmCD34Tx. The data were separately analyzed in the following comparisons: QQMNCTx versus PBMNCTx or IMDM control and QQMNCTx versus GmCD34Tx, eEPCTx, or IMDM control. Especially, vasculogenic properties by transplanted human cells were compared in the groups, excluding IMDM control. qRT-PCR assay to evaluate mRNA expression in ischemic hindlimbs was also implemented simultaneously on the whole groups; the data were analyzed and compared in the same manner as those in the former experiment. Furthermore, in the assay, the ratio of relative mRNA expression of ischemic-to-contralateral (healthy) hindlimbs in IMDM control was compared by Mann-Whitney's U test to confirm the ischemic response. In histological assays, 2 tissue sections per mouse were prepared, and 4 to 6 fields per tissue section were evaluated. Probability values of $P < 0.05$ were deemed statistically significant. All values are expressed as mean \pm SE.

Results

Decrease in Cell Counts in QQMNCs

The fold increase of QQMNCs to PBMNCs per well declined in the whole subjects with an average of 0.54-fold (Table 11). The calculated total QQMNCs derived from 100 mL of PB

Table 11. The Cell and EPC Colony Counts in QQMNC Versus PBMNC

	PB-MNC	QQ-MNC	P Value
Cell counts $\times 10^5$ /well	20.00 \pm 0	10.88 \pm 1.19***	0.0003
Cell counts $\times 10^5$ /100 mL PB	831.3 \pm 75.3	399.2 \pm 43.1***	0.0004
pEPC-CFU counts/ 2 $\times 10^5$ cells/dish	1.58 \pm 0.34	2.89 \pm 0.60*	0.0393
dEPC-CFU counts/ 2 $\times 10^5$ cells/dish	0.71 \pm 0.22	29.41 \pm 2.34***	0.0002
Total EPC-CFU counts/ 2 $\times 10^5$ cells/dish	2.31 \pm 0.53	31.63 \pm 2.66***	0.0002
pEPC-CFU counts $\times 10^5$ /100 mL PB	644.7 \pm 125.2	500.4 \pm 106.2	0.4331
dEPC-CFU counts $\times 10^5$ /100 mL PB	285.1 \pm 78.4	5407 \pm 790.0***	0.0002
Total EPC-CFU counts $\times 10^5$ /100 mL PB	934.3 \pm 190.8	5839 \pm 855.2***	0.0002

Each value indicates a mean \pm SE. N=18 volunteers. dEPC-CFU indicates definitive endothelial progenitor cells colony-forming units; PBMNC, peripheral blood mononuclear cell; pEPC-CFU, primitive endothelial progenitor cells colony-forming units; QQMNC, quality and quantity control culture of mononuclear cell.

* $P < 0.05$; *** $P < 0.001$ versus PBMNC.

decreased from original cells (cell counts $\times 10^5 = 831.3 \pm 75.3$ to 399.2 ± 43.1), on average, by 0.48-fold (Figure 1A; Table 11).

Interestingly, the fold increase of QQMNCs per well exhibited the negative correlation with total cells of PBMNCs from 100 mL of PB in healthy subjects (Figure 1B, left). Taken together, these findings indicate that even using higher PBMNC densities per 100 mL of PB resulted in constant relative yields of QQMNCs per the PB volume (Figure 1B, right).

Increase of Colony-Forming EPCs in QQMNCs

To assess vasculogenic activities between PBMNCs and QQMNCs, EPC-CFA was used to monitor 2 different types of EPC-CFUs, pEPC-CFUs, and dEPC-CFUs, which comprised small cells and large cells, respectively. pEPCs had high cell proliferation activity; in contrast, dEPCs had high vasculogenic potential.¹²

Briefly, for in vitro assays, dEPCs had higher cell adhesion activity than did pEPCs, and dEPCs formed tube-like structures; additionally, dEPCs extensively formed blood vessel de novo after Tx into ischemic hindlimbs of mice, but pEPCs did less.

Therefore, pEPCs derive from relatively immature, highly proliferative EPCs, whereas dEPCs are relatively mature, differentiated, and able to promote EPC-mediated cell functions required for vasculogenesis.

The pEPC and dEPC colony-forming cells (CFCs) each constituted a small proportion of the cells in primary PBMNC populations ($8 \times 10^{-4}\%$ and $3.5 \times 10^{-4}\%$, respectively;

Figure 1C and 1D, left; Table 11). These colony assays demonstrated that QQMNCs have much greater vasculogenic potential than do PBMNCs. After QQ culture, the frequency of total EPC-CFUs from 2×10^5 cells per dish in QQMNCs was significantly enhanced by 13.7-fold of that in PBMNCs. Especially, the frequency of dEPC-CFUs increased by 41.4-fold of that in PBMNCs.

The present data indicate that the vascular regenerative capacity of QQMNCs was superior to that of PBMNCs (Figure 1D, left).

Although QQ culture reduced the count of cells in each individual culture, dEPC-CFCs, and total EPC-CFCs in QQMNCs, derived from the even blood volume were enriched 19.0- and 6.2-fold, relative to those in PBMNCs (Figure 1D, middle; Table 11). Not only were QQ culture enriched with dEPC-CFCs, but also the EPC-CFCs in QQMNCs had a 2.7-fold greater differentiation potential than those in PBMNCs, considering the percentage of dEPC-CFUs to total EPC-CFUs per dish in PBMNCs and QQMNCs (Figure 1D, right).

We also used a linear regression analysis to compare between PBMNCs and QQMNCs with regard to both the quantity and quality of EPC-CFUs (Figure 1E).

Notably, dEPC-CFU and total EPC-CFU counts in QQMNCs were positively correlated with pEPC-CFU counts in PBMNCs, but pEPC-CFU counts in QQMNCs were not (Figure 1E, left). In contrast, neither pEPC-CFU counts nor total EPC-CFU counts in QQMNCs were positively correlated with dEPC-CFU counts in PBMNCs (Figure 1E, middle).

In summary, the frequency of EPC-CFCs in QQMNCs depended on that in PBMNCs (Figure 1E, right). Importantly, the frequency of dEPC-CFCs in QQMNCs was positively correlated with that of pEPC-CFCs in PBMNCs; these correlations indicate that the differentiation during QQ culture of pEPC-CFCs in PBMNCs contributed to formation of dEPC-CFCs in QQMNCs.

Collectively, assays of colony formation demonstrated that the quantitative and qualitative vasculogenic potential of QQMNCs is drastically enhanced, relative to that of PBMNCs, when evaluated even by blood volume.

Moreover, we assessed the functional relationship between CD34⁺ cells and CD34⁺ cell-depleted MNCs (CD34-MNCs) in PBMNCs during QQ culture (Figure 1F). CD34-MNCs after QQ culture (QQ-34-MNCs) did not yield EPC colony, whereas CD34⁺ cells after QQ culture (QQ-34⁺ cells) encompassed pEPC-CFCs. This means that EPC-CFCs were basically derived from CD34⁺ cells. When CD34⁺ cells were cocultured with CD34-MNCs (QQ-34⁺/34-MNC) at a 1:500 ratio, mimicking the proportion of CD34⁺ cells involved in naïve PBMNCs, the dEPC population expanded significantly, relative to the QQ-34⁺ population, even though the original CD34⁺ cell count was equal. The result suggests that CD34-MNCs included some cell population to accelerate EPC expansion and differentiation in CD34⁺ cells through QQ culture.

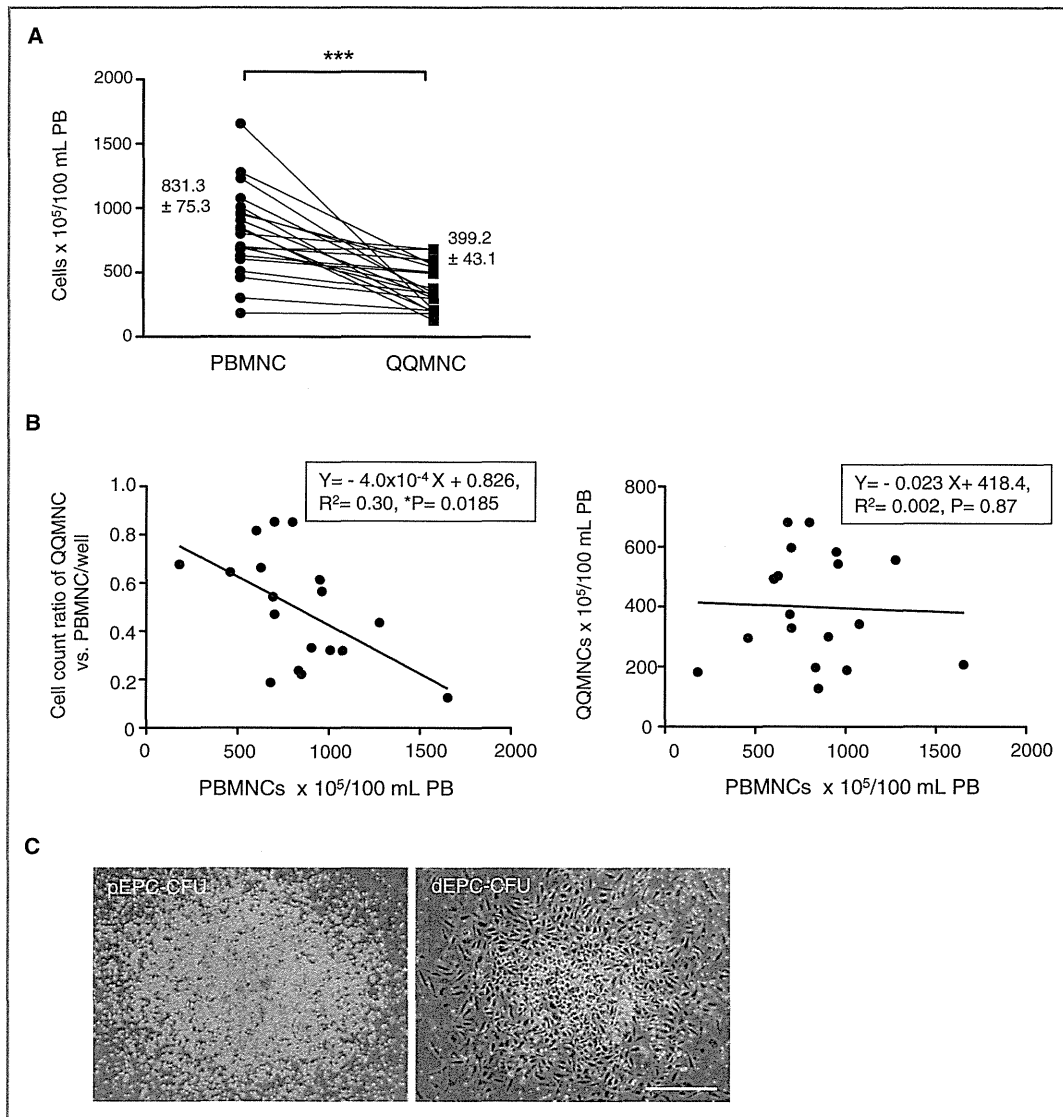


Figure 1. Characteristics of QQMNCs versus PBMNCs. A, The graph shows total cell counts of PBMNCs isolated from 100 mL of PB and the respective QQMNC counts. B, The left graph indicates linear regression analysis between the cell-count ratio of QQMNCs versus PBMNCs (2×10^6 cells/well) and PBMNC counts isolated from 100 mL of PB. The right indicates linear regression analysis of cell counts between PBMNCs and QQMNCs per 100 mL of PB. C, Representative pictures of pEPC-CFU and dEPC-CFU. Scale bar=500 μ m. D, The left and middle graphs are EPC-CFU counts generated from PBMNCs or QQMNCs per dish (2×10^5 cells/dish) and in 100 mL of PB. The right graph shows the percentage of each EPC-CFU count versus total EPC-CFU count per dish. Each column in the graph represents a mean \pm SE. The white and gray areas in the bar graphs indicate the values of pEPC-CFU and dEPC-CFU. E, Linear regression graphs on the interrelation of each EPC-CFU count per dish in QQMNCs to that in PBMNCs. * $P < 0.05$; *** $P < 0.001$. N=18 volunteers. F, Comparison of EPC colony forming activities of post-QQ cultured cells among CD34⁺ cells, CD34-MNCs, and their repopulated cells. QQ-34-MNC: QQ cultured cells of CD34-MNCs (2×10^6 cells/2 mL of QQ culture medium), QQ-34⁺: QQ cultured cells of CD34⁺ cells alone (4×10^3 cells/2 mL of QQ culture medium); QQ-34⁺/34-MNC: QQ cultured cells of CD34⁺ cells repopulated CD34-MNCs (4×10^3 cells for CD34⁺ cells with 2×10^6 cells for CD34-MNCs/2 mL of QQ culture medium). * $P < 0.05$; ** $P < 0.01$; *** $P < 0.001$ versus QQ-34-MNC. # $P < 0.05$; ### $P < 0.001$ versus QQ-34⁺. Each column in the graph represents a mean \pm SE. N=3 volunteers. Aliquots of each cell cultured in the equal volume of QQ culture medium were applied to EPC-CFA; the aliquots were respectively seeded at 2×10^5 cells/dish (3 dishes each for 3 volunteers) for QQ-34-MNC and QQ-34⁺/34-MNC, and at the ratio of 2×10^5 cells to the QQ-34⁺/34-MNCs for QQ-34⁺. dEPC-CFU indicates definitive endothelial progenitor cells colony-forming units; PBMNCs, peripheral blood mononuclear cells; pEPC-CFU, primitive endothelial progenitor cells colony-forming units; QQMNCs, quality and quantity control culture of mononuclear cells.

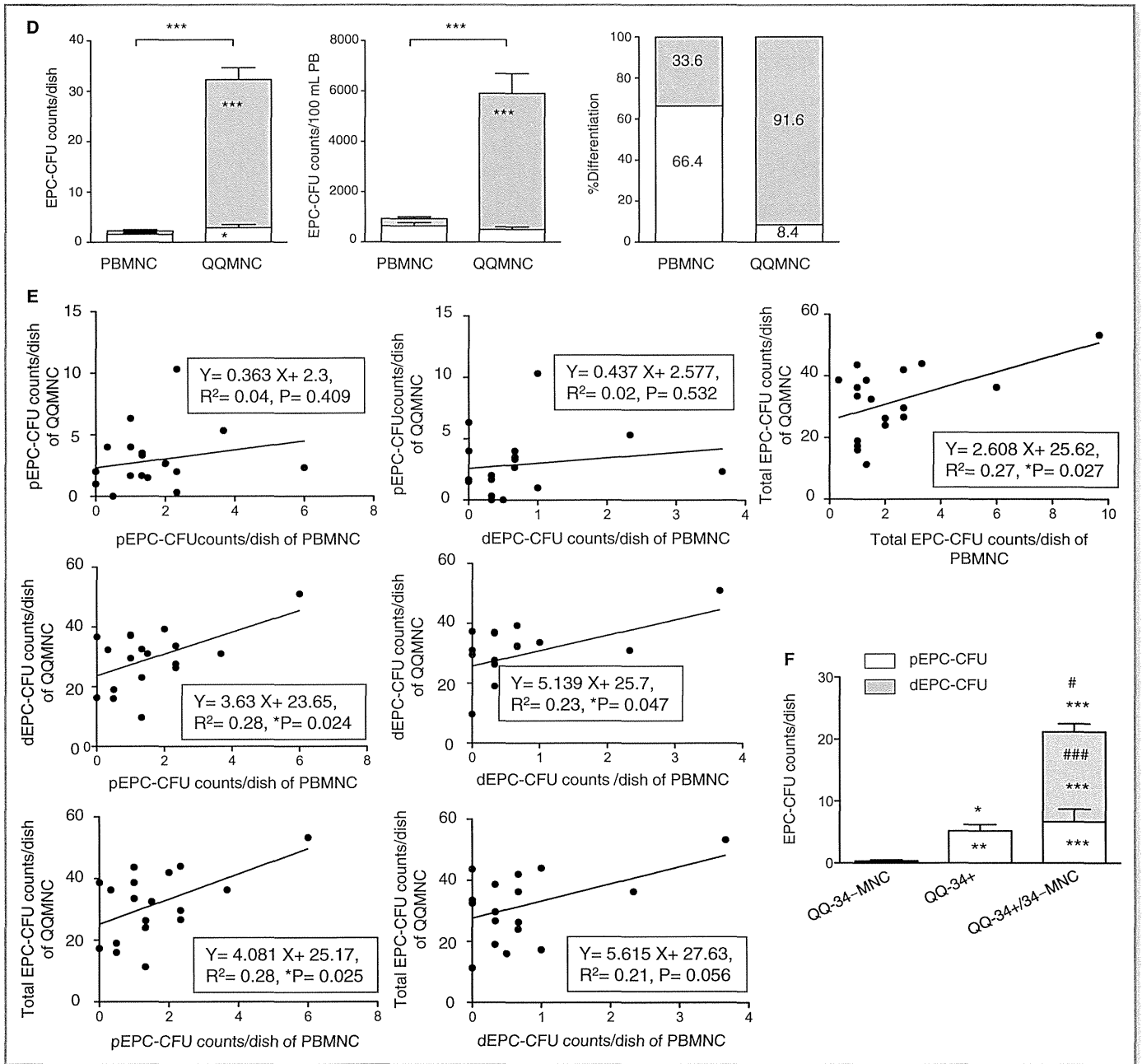


Figure 1. (Continued).

Cell Population Transition in QQMNCs

Based on microscopy and fluorescent cell sorting, large cells were proportionally more common in QQMNC than in PBMNC samples (Figure 2A and 2B). In FCM, the proportion of each positive cell involved in the whole cells of (a), (b), and (c) gates separated with red lines was estimated (Figure 2B).

QQMNCs exhibited the enrichment of CD34⁺ and CD133⁺ stem cell populations, compared to PBMNCs (5.97-fold in CD34⁺ cells; 3.59 in CD133⁺ cells; Figure 2C; Table 12).

In contrast, the proportion of many hematopoietic cell types, including B lymphoid cells (CD19⁺ cells), proinflammatory monocytes/macrophages (CC chemokine receptor 2⁺ cells; CCR2⁺ cells), and natural killer (NK) cells (CD56⁺ cells) was lower in QQMNC than in PBMNC samples.

The proportion of endothelial lineage cells was slightly increased in CD105, whereas it was not changed in CD31 and slightly decreased in vWF. Although not significant, the proportion was slightly increased in CD146, while decreased in VEGF receptor (VEGFR)-2.

In the T-lymphoid cell population, and particularly in the angiogenic T-cell subpopulation, C-X-C chemokine receptor

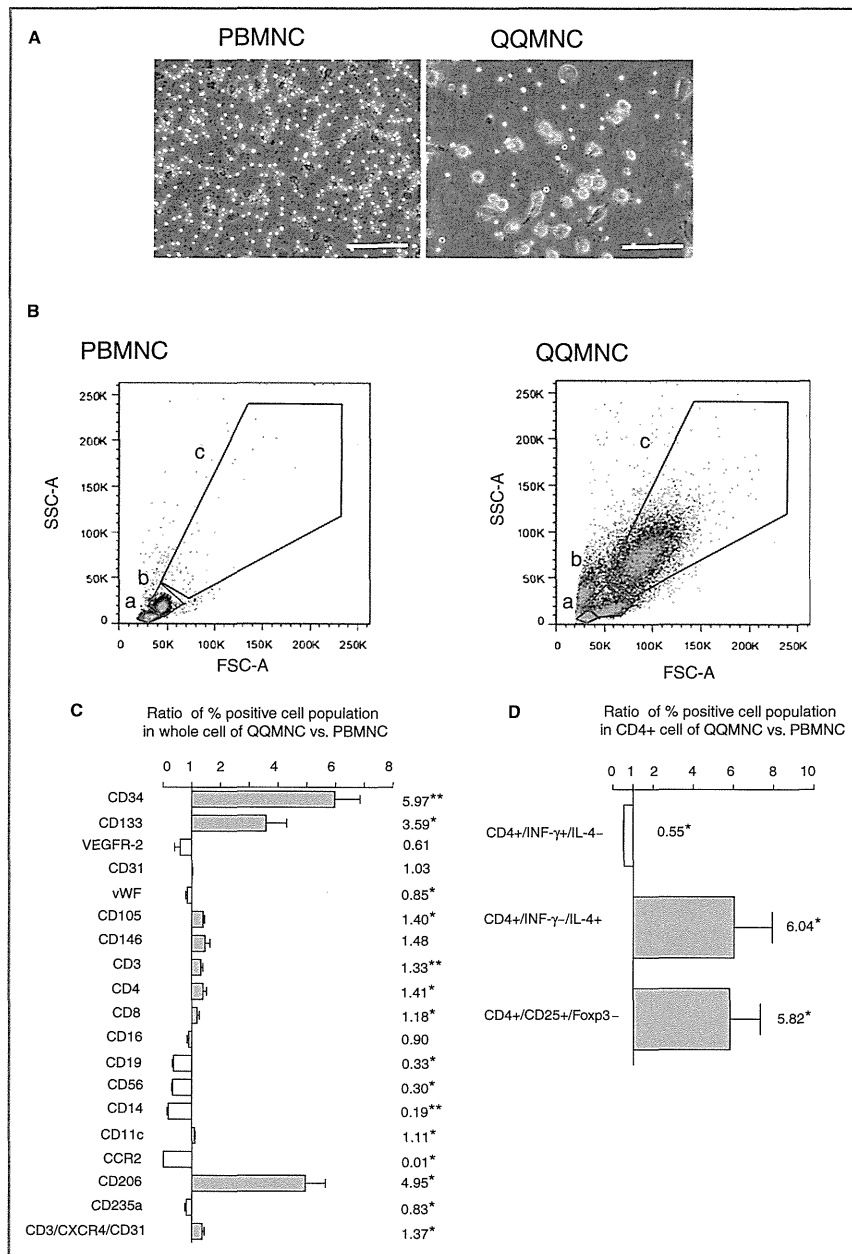


Figure 2. Flow cytometry analysis of PBMNCs and QQMNCs. A, Representative features of PBMNCs at 3 hours after seeding and QQMNCs after 7 days. Scale bar=100 μm. B, Scatter diagrams of PBMNCs and QQMNCs in flow cytometry. The red lines indicate the cellular-sized gates of lymphocyte (a), monocyte (b), or the larger cell (c). C, The bar graph shows the ratio of each percent (%) cell positivity in QQMNCs to that in PBMNCs. N=4 to 6 volunteers. The investigated cell surface markers were as follows: hematopoietic stem cell (CD34, CD133), endothelial cell (VEGFR-2, CD31, vWF, CD105, and CD146), T cell (CD3, CD4, CD8, and CD3/CXCR4/CD31), NK cell (CD16 and CD56), B cell (CD19), monocyte (CD14), dendritic cell (CD11c), M1 macrophage (CCR2), M2 macrophage (CD206), and erythroid progenitor (CD235a). D, The bar graph indicates the ratio of each % helper T subset positivity in CD4⁺ cells of QQMNCs to that of PBMNCs. N=6 volunteers. **P*<0.01; ***P*<0.01 in (C and D). The gray or white column represents a mean±SE in each increase or decrease. The number associated with each graph column shows the mean value. CCR2 indicates CC chemokine receptor 2; Foxp3, forkhead box P3; FSC-A, forward scatter-area; IL, interleukin; INF, interferon; NK, natural killer; PBMNCs, peripheral blood mononuclear cells; QQMNCs, quality and quantity control culture of mononuclear cells; SSC-A, side scatter-area; VEGFR, vascular endothelial growth factor receptor; vWF, von Willebrand factor.

Table 12. Percent Positivities of Hematopoietic Cell Populations in QQMNC Versus PBMC

	% in PBMC	% in QQMNC	<i>P</i> Value	Ratio	<i>P</i> Value
CD34 ⁺	0.21±0.03	1.25±0.26**	0.0078	5.97±0.88**	0.0078
CD133 ⁺	0.23±0.08	0.48±0.08	0.0977	3.59±0.71*	0.0195
VEGFR-2 ⁺	1.07±0.15	0.67±0.28	0.2500	0.61±0.21	0.2500
CD31 ⁺	39.60±1.93	40.66±1.89	0.2969	1.03±0.02	0.2969
vWF ⁺	10.52±3.63	10.33±4.07	0.7422	0.85±0.06*	0.0391
CD105 ⁺	22.65±1.37	32.05±2.84*	0.0313	1.40±0.05*	0.0313
CD146 ⁺	1.57±0.20	2.09±0.16	0.1094	1.48±0.17	0.1094
CD3 ⁺	55.16±4.12	71.30±2.61**	0.0078	1.33±0.08**	0.0078
CD4 ⁺	34.38±4.27	46.38±3.28*	0.0350	1.41±0.12*	0.0313
CD8 ⁺	19.54±2.70	22.03±1.80*	0.0345	1.18±0.08*	0.0313
CD16 ⁺	35.66±1.73	31.76±0.88	0.2500	0.90±0.06	0.2500
CD19 ⁺	22.00±2.27	6.98±0.16*	0.0350	0.33±0.03*	0.0313
CD56 ⁺	24.50±1.17	7.63±1.11*	0.0350	0.30±0.03*	0.0313
CD14 ⁺	19.80±1.73	3.47±0.57**	0.0078	0.19±0.04**	0.0078
CD11c ⁺	35.81±2.19	39.57±2.39*	0.0391	1.11±0.03*	0.0391
CCR2 ⁺	15.70±1.48	0.22±0.06*	0.0350	0.01±0.004*	0.0355
CD206 ⁺	5.53±0.33	26.28±2.69*	0.0350	4.95±0.70*	0.0355
CD235a ⁺	0.88±0.09	0.71±0.03*	0.0211	0.83±0.05*	0.0223
CD3 ⁺ /CXCR4 ⁺ /CD31 ⁺	30.28±1.75	41.01±2.07*	0.0350	1.37±0.07*	0.0350

"% in PBMC" and "% in QQMNC" indicate the % positivity of each cell population in the whole cell of QQMNC and PBMC. "Ratio" means the ratio of the % positivity in the whole cell of QQMNC to that of PBMC, corresponding to Figure 2C. The left *P* values indicate the comparison of % cell positivities between QQMNC and PBMC; the right ones indicate that of the ratios. N=4 to 6 volunteers. CCR2 indicates CC chemokine receptor 2; CXCR4, C-X-C chemokine receptor type 4; PBMC, peripheral blood mononuclear cell; QQMNC, quality and quantity control culture of mononuclear cell; VEGFR, vascular endothelial growth factor receptor; vWF, von Willebrand factor.

P*<0.05; *P*<0.01 versus PBMC.

type 4 (CXCR4⁺/CD31⁺/CD3⁺ cells³⁰ increased significantly after QQ culture. Notably, the proportion of anti-inflammatory M2-type (CD206) cells increased significantly (4.95-fold) in the 2 categories of macrophages; inversely, the proportion of proinflammatory M1-type (CCR2) cells decreased significantly (0.01-fold).^{31,32}

More interestingly, when activated T lymphocytes of QQMNCs or PBMCs by PMA and ionomycin, the proportion of Th1 cells (CD4⁺/INF-γ⁺/IL-4⁻) in helper T (CD4⁺) cells in

QQMNCs declined 0.55-fold of that in PBMCs. In contrast, the proportions of Th2 cells (CD4⁺/INF-γ⁻/IL-4⁺) and regulatory T cells (CD4⁺/CD25⁺/Foxp3⁺) increased 6.04- and 5.82-fold (Figure 2D; Table 13).

These data indicate that QQ culture conditions specifically selected for and/or promote proliferation of stem/progenitor cell populations of EPCs as well as anti-inflammatory and angiogenic monocytes/T-lymphocytes in primary PBMC cultures.

Table 13. Percent Positivities of Helper T-Cell Subsets in CD4⁺ T Cells of QQMNC Versus PBMC

	% in CD4 ⁺ Cell				
	PBMC	QQMNC	<i>P</i> Value	Ratio	<i>P</i> Value
CD4 ⁺ /INF-γ ⁺ /IL-4 ⁻	10.34±3.71	5.90±2.28*	0.0355	0.55±0.02*	0.0355
CD4 ⁺ /INF-γ ⁻ /IL-4 ⁺	2.94±0.53	14.91±3.10*	0.0355	6.04±1.90*	0.0350
CD4 ⁺ /CD25 ⁺ /Foxp3 ⁺	3.40±0.82	15.00±1.96*	0.0355	5.82±1.51*	0.0355

"% in CD4⁺ cell" indicates the percent (%) positivity of each helper T subset in CD4⁺ T cell of QQMNC and PBMC. "Ratio" means the ratio of the % positivity in CD4⁺ T cell of QQMNC to that of PBMC, corresponding to Figure 2D. The left *P* values indicate the comparison of % cell positivities between QQMNC and PBMC; the right ones indicate that of the ratios. Foxp3 indicates forkhead box P3; IL, interleukin; INF, interferon; PBMC, peripheral blood mononuclear cell; QQMNC, quality and quantity control culture of mononuclear cell. N=6 volunteers. **P*<0.05 versus PBMC.

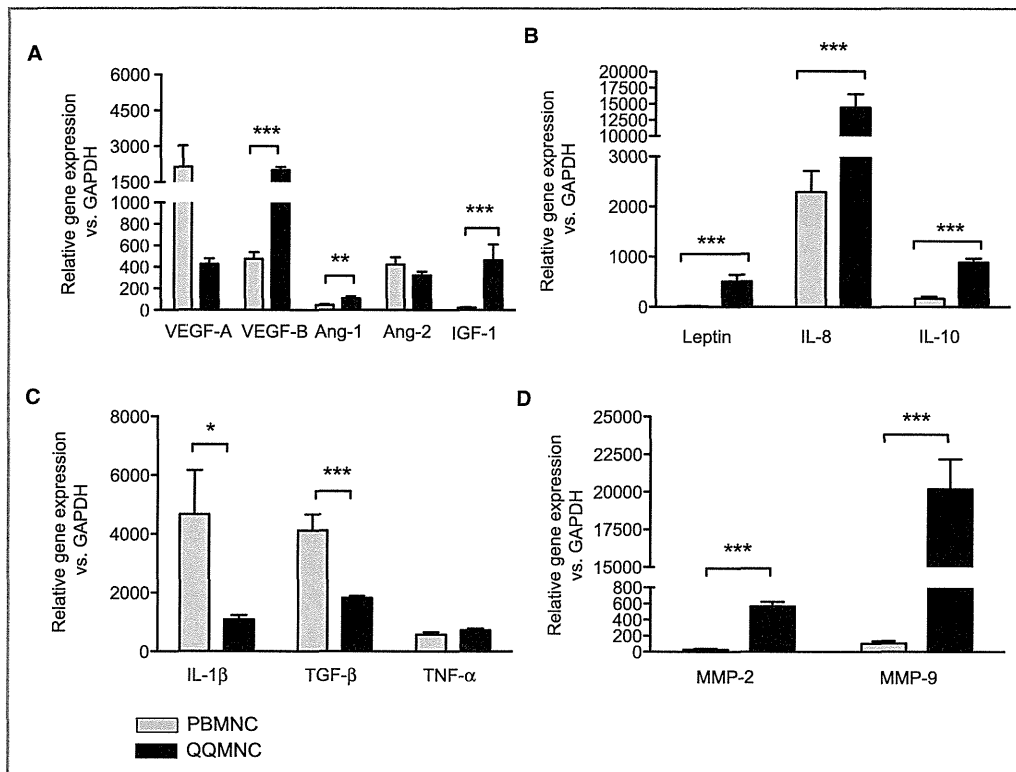


Figure 3. qRT-PCR assay of PBMNCs and QQMNCs. A, Proangiogenic growth factors. B, Proangiogenic cytokines. C, Pro- or anti-inflammatory cytokines. D, MMPs. * $P < 0.05$; ** $P < 0.01$; *** $P < 0.001$. Each graph column represents a mean \pm SE. $N = 8$ volunteers. Ang indicates angiotensin; GAPDH, glyceraldehyde-3-phosphate dehydrogenase; IGF, insulin-like growth factor; IL, interleukin; MMPs, matrix metalloproteinases; PBMNCs, peripheral blood mononuclear cells; QQMNCs, quality and quantity control culture of mononuclear cells; qRT-PCR, quantitative real-time polymerase chain reaction; TGF, transforming growth factor; TNF, tumor necrosis factor; VEGF, vascular endothelial growth factor.

Enhanced Gene Expression for Vascular Regeneration and Anti-Inflammation in QQMNCs

Expression of genes encoding vascular regeneration factors, including VEGF-B, angiotensin-1 (Ang-1), leptin, IL-8, IL-10, and insulin-like growth factor 1 (IGF-1), was much higher in QQMNCs than in PBMNCs; the fold increases in QQMNCs versus PBMNCs were 4.2 for VEGF-B, 2.4 for Ang-1, 35.9 for leptin, 6.3 for IL-8, 5.4 for IL-10, and 21.2 for IGF-1 (Figure 3A and 3B). Especially, VEGF-B and Ang-1 also induce vascular maturation,^{33,34} and IGF-1 exerts myogenic potential.³⁵

Additionally, expression of the gene encoding IL-1 β , a proinflammatory cytokine, in QQMNCs decreased by 0.23-fold of that in PBMNCs, with the increase of the gene encoding the anti-inflammatory IL-10 (Figure 3C). These expressional profiles indicate that QQMNCs preferred to arrange an anti-inflammatory environment in injured tissue. Furthermore, the expression of genes encoding to matrix metalloproteinases (MMPs) of MMP-2 and -9 was significantly higher in QQMNCs

than in PBMNCs; the fold increases were 22.1 for MMP-2 and 189.4 for MMP-9 (Figure 3D). MMP-2 and -9 have antifibrotic activity that plays critical roles during neovascularization and tissue remodeling.^{36,37}

QQMNCs Promote Angiogenesis In Vitro

Using an in vitro Matrigel assay, we found that QQMNCs promoted tube formation of cocultured HUVECs for 12 hours, but PBMNCs did not (tube counts/ $\times 2$ HPF = 63.3 ± 1.43 for HUVEC+QQMNC versus 55.1 ± 1.45 for HUVEC+PBMNC or 55.3 ± 1.39 for HUVEC alone; Figure 4A and 4B).

Moreover, QQMNCs were readily incorporated into the tubes formed by HUVECs; in contrast, PBMNCs were rarely incorporated into such tubes (incorporated DiI-uptaking cells in tubes/ $\times 4$ HPF = 38.5 ± 8.30 for QQMNC versus 8.72 ± 1.89 for PBMNC; Figure 4C and 4D).

These findings indicate that in vitro QQMNCs had more angiogenic- and EPC-incorporating activity than did PBMNCs.

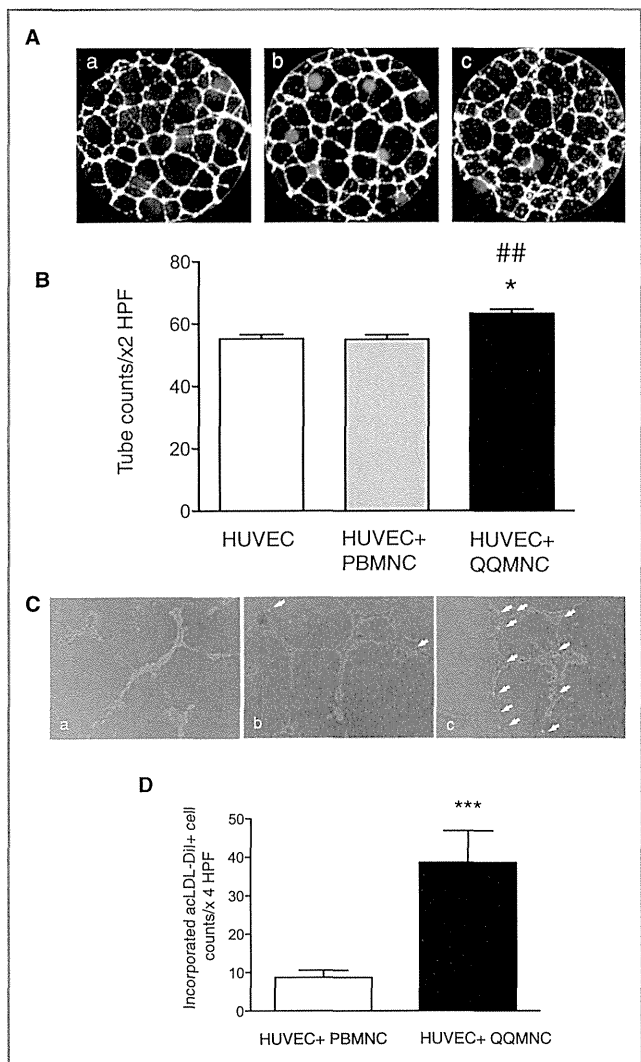


Figure 4. In vitro angiogenic assay of HUVECs cocultured with QQMNCs. A, Features of tubes formed by HUVECs. B, The bar graphs represent the number of tubes counted under $\times 2$ HPF. $*P < 0.05$ versus HUVEC; $##P < 0.01$ versus HUVEC+PBMNC. C, Incorporation of acLDL-Dil uptaking PBMNCs or QQMNCs into tubes of HUVECs. Arrow heads indicate PBMNCs or QQMNCs that are labeled with acLDL-Dil and incorporated into tubes formed by HUVECs. (a) HUVEC alone, (b) HUVEC+PBMNC, and (c) HUVEC+QQMNC in (A and C). D, The bar graphs show numbers of incorporated PBMNCs or QQMNCs, counted under $\times 4$ HPF. $***P < 0.001$. Each graph column represents a mean \pm SE. $N = 10$ wells/group. acLDL-Dil indicates acetylated low density lipoprotein, labeled with 1,1'-dioctadecyl-3,3,3',3'-tetramethyl-indocarbocyanine perchlorate; HPF, high power field; HUVECs, human umbilical vein endothelial cells; PBMNCs, peripheral blood mononuclear cells; QQMNCs, quality and quantity control culture of mononuclear cells.

Physiological Recovery of Blood Perfusion in Ischemic Hindlimb After QQMNCtx

We investigated the potential of QQMNCs to treat ischemia, using a mouse ischemic hindlimb model; the effect was

evaluated by blood flow measurement for 21 days after ischemic surgery. We compared the effect of QQMNCtx with that of no-cell Tx (IMDM medium-injected mice:IMDM control) or PBMNCtx (Figure 5A).

For each mouse, we measured blood flow in the ischemic and contralateral hindlimb; we then calculated the ratio of ischemic blood flow to contralateral flow: % blood flow ratio in the QQMNCtx, PBMNCtx, and control groups—at day 14, 48.8 ± 4.25 , 32.3 ± 5.53 , and 28.9 ± 4.52 ; at day 21, 50.7 ± 5.50 , 28.1 ± 6.19 , and 27.4 ± 6.98 , respectively. The ratio in the QQMNCtx was significantly higher after day 14 than that in PBMNCtx and control, indicating that QQMNCtx recovered ischemic blood flow greater than the others.

Comparing to other EPC transplantations (Figure 5B), QQMNCtx improved the blood-flow ratio earlier than GmCD34Tx, eEPCTx, and control: % blood flow ratio in QQMNCtx, GmCD34Tx, eEPCTx, and control—at day 14, 52.8 ± 6.13 , 37.6 ± 3.48 , 24.8 ± 2.83 , and 24.1 ± 5.13 ; at day 21, 62.1 ± 6.61 , 53.9 ± 6.18 , 31.8 ± 1.57 , and 27.7 ± 3.86 , respectively.

The % ratios of autoamputation in the QQMNCtx, PBMNCtx, and control groups were 4.3, 9.5, and 15.8, respectively; conversely, those of limb salvage were 21.7, 9.5, and 10.5, respectively. These findings indicate that QQMNCtx potentiated physiological recovery in hindlimb ischemia more so than did PBMNCtx or control (Figure 5C).

When compared to GmCD34Tx and eEPCTx, the % ratios of autoamputation in QQMNCtx, GmCD34Tx, and eEPCTx were 4.5, 26.3, and 37.5, respectively. In contrast, those of limb salvage in QQMNCtx, GmCD34Tx, and eEPCTx were 27.3, 21.1, and 25.0, respectively.

Regarding these findings, the earlier blood flow recovery by QQMNCtx might favorably rescue the ischemic foot from injury, compared to other treatments (Figure 5D).

QQMNCtx Potentiates Vascular and Muscle Regeneration in Ischemic Hindlimb

Angiogenesis and arteriogenesis

For each animal, we used histological methods to measure Isolectin B4-FITC stained microvessel density and assess angiogenic capacity in the ATM of ischemic hindlimbs; the mean densities (microvessel counts/ mm^2) for the QQMNCtx, PBMNCtx, and control groups were 400.7 ± 37.9 , 118.9 ± 20.1 , and 98.7 ± 15.8 , respectively (Figure 6A and 6B).

We also evaluated pericyte-recruited (α -SMA⁺) microvessel density in the ATM to assess arteriogenesis for vascular maturation: The mean densities (pericyte-recruited microvessel counts/ mm^2) for the QQMNCtx, PBMNCtx, and control groups were 38.7 ± 5.5 , 19.8 ± 4.3 , and 15.0 ± 2.7 , respectively (Figure 6A and 6C).

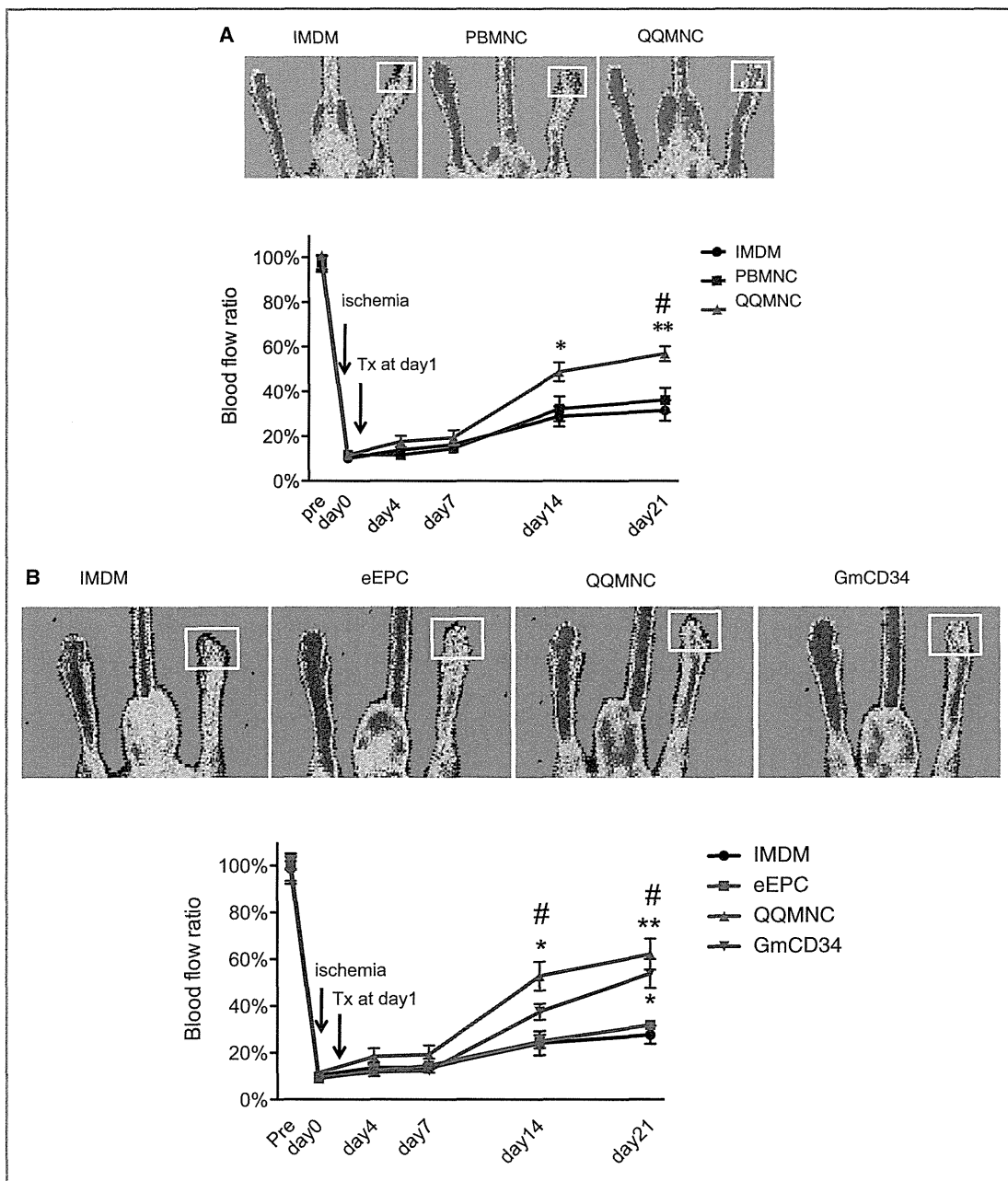


Figure 5. Blood flow and distribution of limb salvage patterns in ischemic hindlimbs. A and B, Laser Doppler imaging was used to analyze blood flow 21 days after ischemia. Cells were transplanted at 1×10^4 /mouse (5×10^3 cells/each of ATM and GCM). The top panels show the representative features in each group. ROI for blood flow measurement is shown by a yellow square. The bottom line graph presents percent (%) blood-flow ratio of ischemic-to-contralateral hindlimb during the observation period for 21 days. * $P < 0.05$; ** $P < 0.01$ versus IMDM control. # $P < 0.05$ versus PBMNCTx in (A) or eEPCTx in (B). Each line graph represents a mean \pm SE. N=12 mice/group. C and D, Limb salvage features of QQMNCTx versus PBMNCTx day 21 after ischemia. The top pictures in (C) show the representative features of ischemic leg patterns; the severity of the phenotypes are graded from the left to the right. The column graphs in (C and D) show the respective % distributions of severity for each group. N=19 mice for IMDM control, 21 for PBMNCTx, and 23 for QQMNCTx in (C). N=10 mice per each group in (D). LS, limb salvage; TN, toe necrosis; FN, foot necrosis; AA, autoamputation in (C and D). ATM indicates anterior tibial muscle; eEPCTx, early endothelial progenitor cell transplantation; GCM, gastrocnemius muscle; GmCD34, granulocyte colony-stimulating factor mobilized CD34⁺ cell; IMDM, Iscove's Modified Dulbecco's Medium; PBMNCTx, peripheral blood mononuclear cell transplantation; QQMNCTx, quality and quantity control culture of mononuclear cell transplantation; ROI, regions of interest.

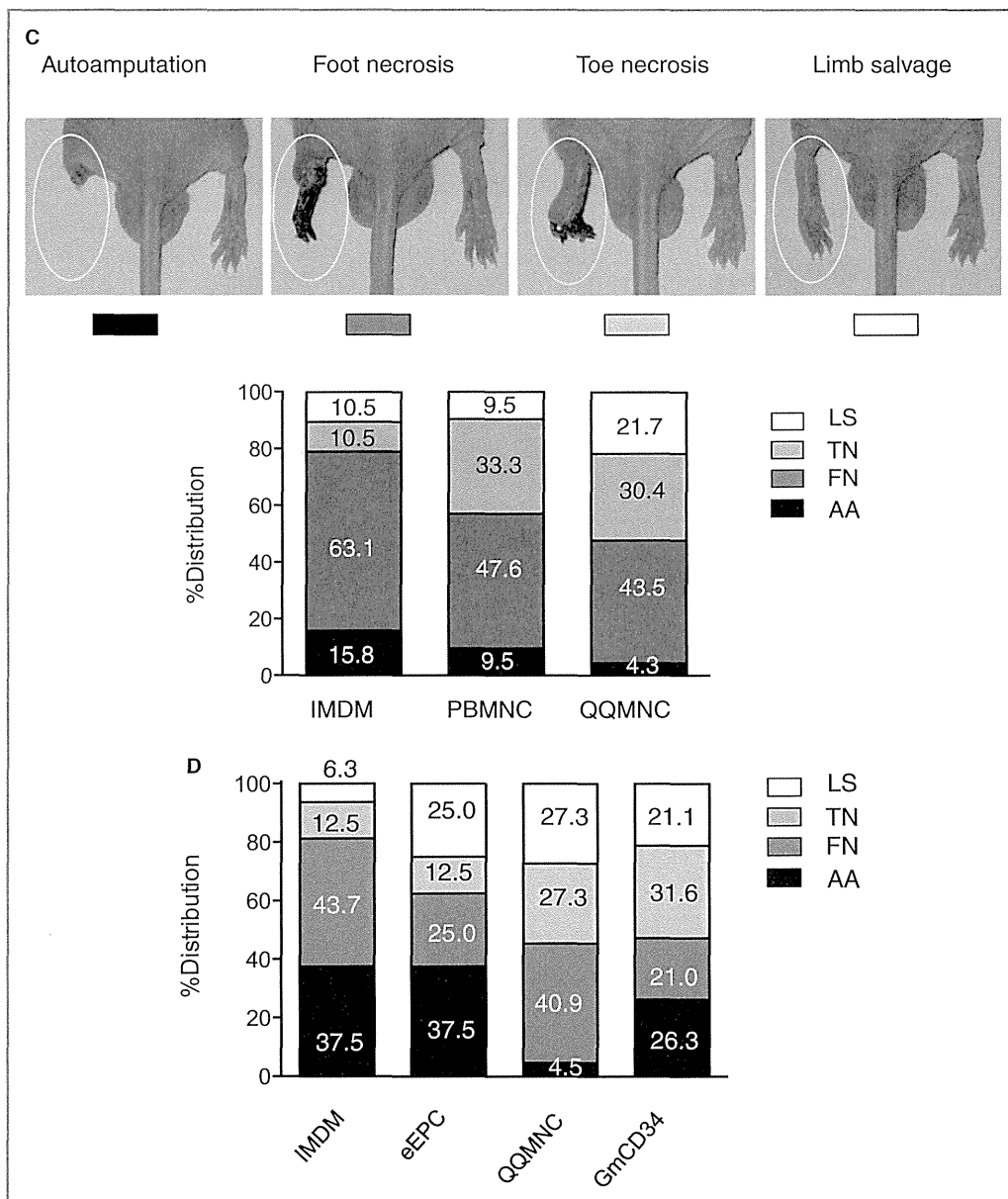


Figure 5. (Continued).

Likewise, the mean microvessel densities (microvessel counts/mm²) for the QQMNCtx, GmCD34Tx, eEPCTx, and control groups were 510.7±30.0, 430.6±29.8, 347.9±36.5, and 210.5±16.8 respectively (Figure 6D and 6E). The mean pericyte-recruited microvessel densities (pericyte-recruited microvessel counts/mm²) for the QQMNCtx, GmCD34Tx, eEPCTx, and control groups were 42.6±4.3, 39.5±3.8, 29.8±2.0, and 23.2±2.9, respectively (Figure 6D and 6F). These findings demonstrate that QQMNCtx promoted angiogenesis and arteriogenesis for vascular maturation.

Vasculogenesis

We performed in vivo experiments to assess vasculogenic properties of transplanted cells (2×10⁵ cells/mouse): to investigate

whether and to what extent transplanted cells differentiate into endothelial cell forming vascular structure in the host tissue, using a confocal fluorescence microscope (Figure 7A; Video S1).

IHC stainings demonstrated the significantly higher vasculogenic microvessel counts in QQMNCtx muscles than those in PBMNCtx (Figure 7B through 7D; Table 14).

The average vasculogenic microvessel densities in 2D image (vasculogenic microvessel counts/mm²) for the QQMNCtx and PBMNCtx groups were 811.6±178.6 and 202.9±97.3 (Figure 7C); the % ratios of vasculogenic microvessel volume per image cube for the respective groups were 0.76±0.17 and 0.05±0.04 (Figure 7D).

The potential of QQMNCtx was also markedly superior to that of eEPCTx, whereas it was equal to or greater than that of

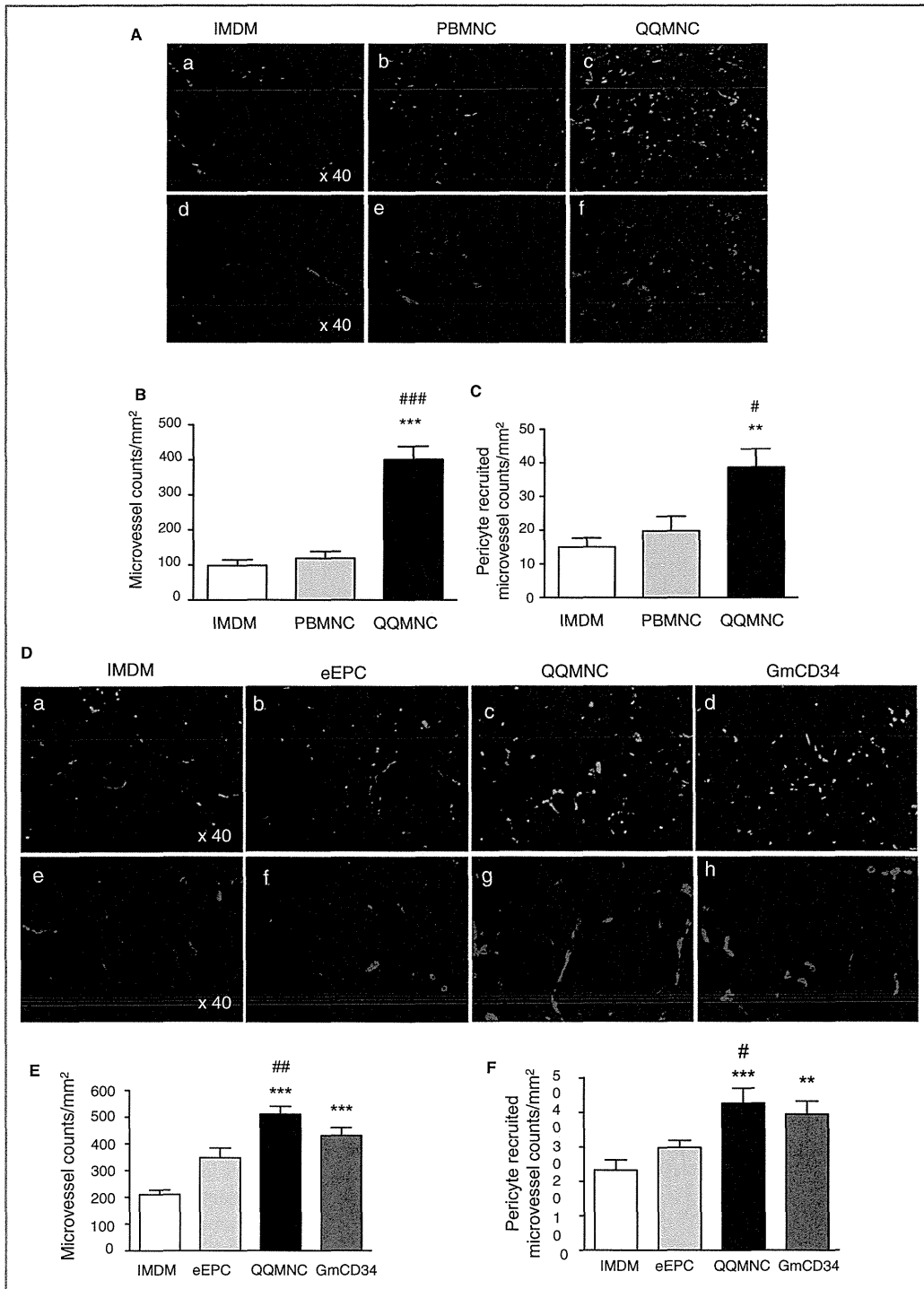


Figure 6. Assessment of angiogenesis and arteriogenesis in ischemic hindlimbs. A and D, Representative pictures of angiogenesis and arteriogenesis in ATM in each group. (a through c) in (A) and (a through d) in (D): mouse microvessels stained with isolectin B4-FITC. (d through f) in (A) and (e through h) in (D): pericyte recruited microvessels stained with Cy3-conjugated anti- α -SMA antibody. The graphs present the counts of microvessels in (B and E) and pericyte recruited microvessels in (c and f). * P <0.05; ** P <0.01; *** P <0.001 versus IMDM control in (B, C, E, and F). # P <0.05; ### P <0.001 versus PBMNCTx in (B and C). # P <0.05; ## P <0.01 versus eEPCtx in (E and F). $\times 40$ HPF. Each column in the graph represents a mean \pm SE. N=6 mice per group. ATM indicates anterior tibial muscle; eEPCtx, early endothelial progenitor cell transplantation; FITC, fluorescein isothiocyanate; GmCD34, granulocyte colony stimulating factor mobilized CD34⁺ cell; HPF, high power field; PBMNCTx, peripheral blood mononuclear cell transplantation; QQMNC, quality and quantity control culture of mononuclear cells; α -SMA, alpha-smooth muscle actin.

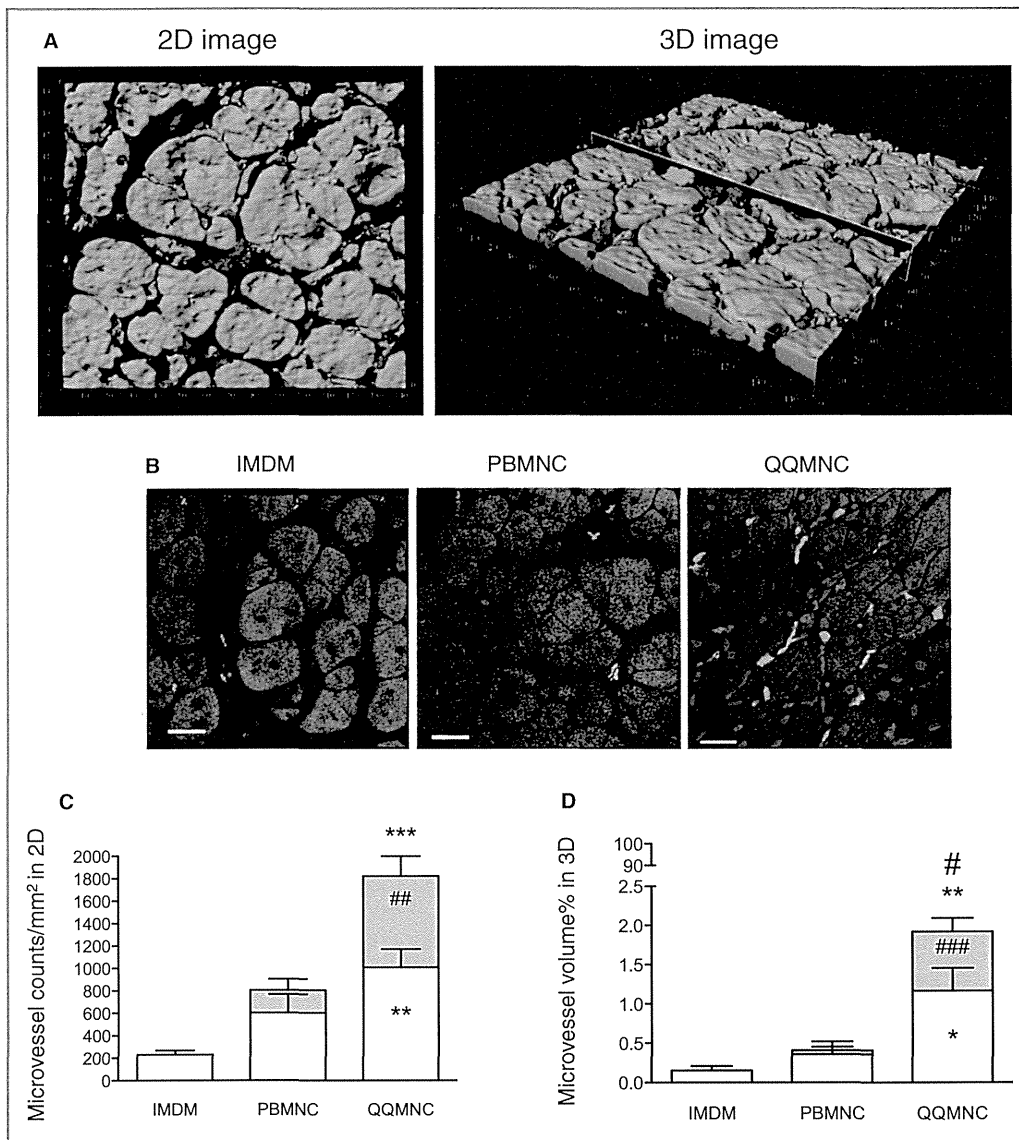


Figure 7. Evaluation of vasculogenesis by transplanted cells in ischemic hindlimbs. A, The representative 2D and 3D images to assess vasculogenesis and angiogenesis in cell (GmCD34) transplanted ATM by 3D spectrum analysis using a confocal microscope. (Green) Mouse microvessels stained with isolectin B4-FITC, (red) vasculogenic microvessels by transplanted human cells, stained with human specific anti-CD31 antibody/Alexa 594, and (blue) nuclei stained with TOTO-3. The unit of numbers in their images indicates micrometers (μm). B and E, The panels show the representative similar images in each treatment group. Cells were transplanted at 2×10^5 cells per ATM. Scale bar=20 μm . C and F, Microvessel counts/mm² in each group. D and G, Percent (%) microvessel volume per 3D image cube ($142.58 \times 142.58 \times 8 \mu\text{m}^2$) in each group. * $P < 0.05$; ** $P < 0.01$; *** $P < 0.001$ versus IMDM control in (C, D, F, and G). # $P < 0.05$; ### $P < 0.01$; #### $P < 0.001$ versus PBMNCTx in (C and D) or eEPCTx in (F and G). Each column on the graph represents a mean \pm SE. N=3 to 4 mice per group. ATM indicates anterior tibial muscle; eEPCTx, early endothelial progenitor cell transplantation; GmCD34, granulocyte colony-stimulating factor mobilized CD34⁺ cell; PBMNCTx, peripheral blood mononuclear cell transplantation; QQMNC, quality and quantity control culture of mononuclear cells.

GmCD34Tx. The average vasculogenic microvessel densities (vasculogenic microvessel counts/mm²) for the GmCD34Tx and eEPCTx groups were 662.2 ± 98.6 and 203.8 ± 50.8 , respectively (Figure 7E and 7F; Table 14); the % ratios of vasculogenic microvessel volume per image cube for the

groups were 0.53 ± 0.15 and 0.06 ± 0.02 (Figure 7E and 7G; Table 14).

Similarly, the angiogenic properties of transplanted cells, here evaluated by the confocal microscopic analysis, exhibited the compatible feature with those in the aforementioned

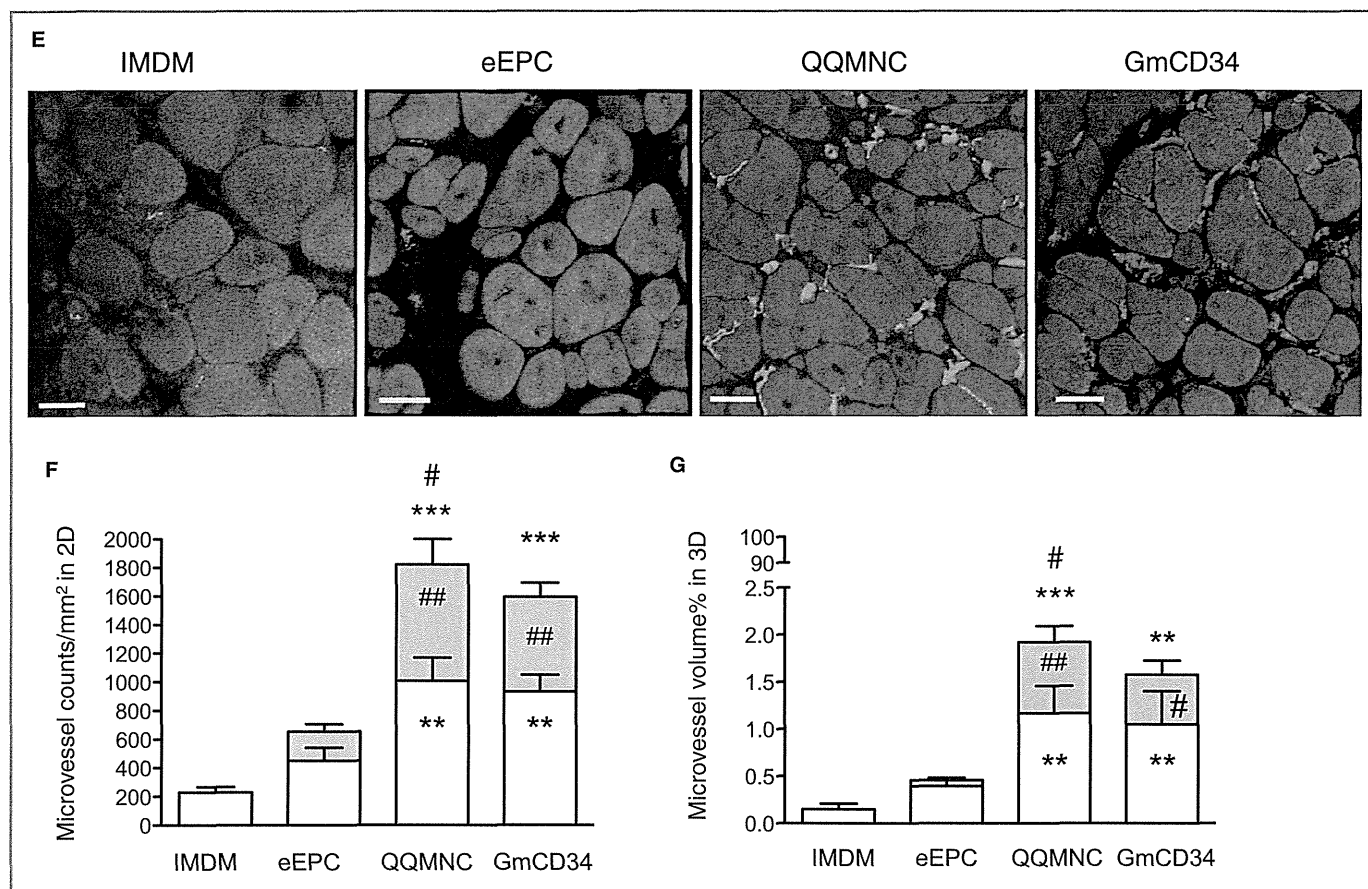


Figure 7. (Continued).

experiments of the low-dose cellular Tx (1×10^4 cells/mouse).

The findings indicate that transplanted cells of QQMNCs, as well as GmCD34, exerted vasculogenic properties in ischemic hindlimbs superior to those of PBMNCs or eEPCs.

Myogenesis

Muscle fibers with centrally located nuclei indicate myogenesis mediated by fusion of myoblasts in ATM of ischemic

hindlimbs; therefore, we determined that the average densities of such regenerating muscle fibers (regenerating muscle fibers/mm²) for the QQMNCtx, PBMNCtx, and control groups were 775.6 ± 113.3 , 424.2 ± 47.12 , and 398.6 ± 48.42 , respectively (Figure 8A and 8B).

In the respective experiments to compare myogenesis among the QQMNCtx, GmCD34Tx, eEPCTx, and control groups, we also determined that the average densities of regenerating muscle fibers (regenerating muscle fiber counts/

Table 14. The Angiogenic and Vasculogenic Microvessels in Ischemic ATMs 21 Days After Surgery

Tx Cells	Microvessel counts/mm ² in 2D			Microvessel Volume % in 3D		
	Angio	Vasculo	Total	Angio	Vasculo	Total
IMDM	229.6±37.4	0±0	229.6±37.4	0.15±0.06	0±0	0.15±0.06
PBMNC	602.6±165.4	202.9±97.3	805.5±220.6	0.36±0.16	0.05±0.04	0.41±0.19
eEPC	449.7±90.7	203.8±50.8	653.5±115.5	0.39±0.07	0.06±0.02	0.46±0.07
QQMNC	1008.0±162.1	811.6±178.6	1820.0±191.0	1.17±0.29	0.76±0.17	1.92±0.37
GmCD34	930.8±118.2	662.2±98.6	1593.0±168.7	1.05±0.35	0.53±0.15	1.58±0.46

Each value indicates a mean±SE. N=3 to 4 mice per group. Angio indicates angiogenic microvessel; ATM, anterior tibial muscle; eEPC, early endothelial progenitor cell; GmCD34, granulocyte colony-stimulating factor mobilized CD34⁺ cell; PBMNC, peripheral blood mononuclear cell; QQMNC, quality and quantity control culture of mononuclear cell; Tx cells= 2×10^5 cells/mouse transplanted into ischemic ATM; Vasculo, vasculogenic microvessel.

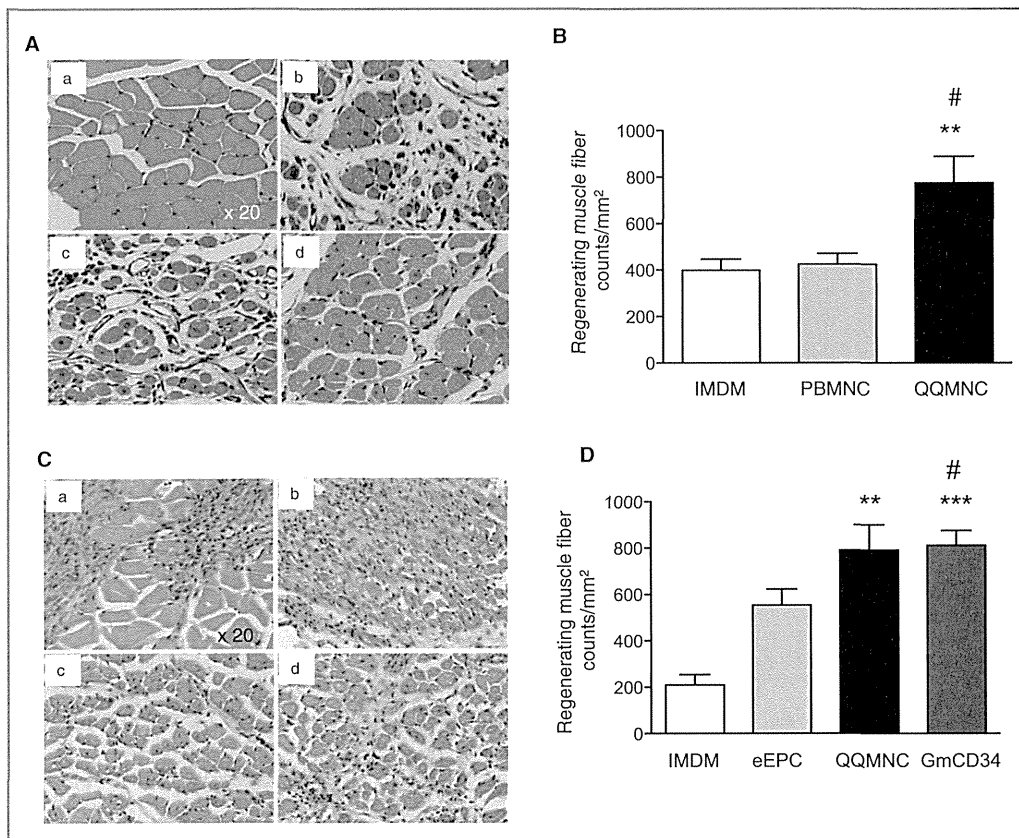


Figure 8. Histological evaluation of myogenesis in ischemic hindlimbs. A and C, Representative images of muscle tissues in ATM by H&E staining. (a) Normofused tissue with normal morphology of skeletal muscle fibers with the subsarcolemmal nuclei in contralateral hindlimb of IMDM control, (b) ischemic hindlimbs from IMDM control, (c) PBMNCTx, or (d) QQMNTx in (A). (a) IMDM control, (b) eEPCTx, (c) QQMNTx, and (d) GmCD34Tx in (C). Note that the smaller size of the fibers in combination with centrally located nuclei indicated that a muscle fiber had been actively regenerating. B and D, The graphs present the counts of regenerating muscle fibers in each group. $**P < 0.01$; $***P < 0.001$ versus IMDM control in (B and D). $\#P < 0.05$ versus PBMNCTx in (B) or eEPCTx in (D). Each column in the graph represents a mean \pm SE. $\times 20$ HPF. $N = 6$ mice per group. ATM indicates anterior tibial muscle; eEPCTx, early endothelial progenitor cell transplantation; GmCD34, granulocyte colony-stimulating factor mobilized CD34⁺ cell; H&E, hematoxylin and eosin; HPF, high power field; PBMNCTx, peripheral blood mononuclear cell transplantation; QQMNTx, quality and quantity control culture of mononuclear cell transplantation.

mm²) for the respective groups were 790.7 ± 110.1 , 811.8 ± 63.6 , 553.6 ± 69.25 , and 209.4 ± 44.01 , respectively (Figure 8C and 8D). These findings indicate that QQMNTx potentiated myogenesis greater than PBMNCTx and control, or equal to GmCD34Tx in ischemic hindlimbs, although did not compare to eEPCTx.

Inhibitory Effects of QQMNTx to Fibrosis and Inflammation in Hindlimb Ischemia

To evaluate anti-inflammatory and -fibrotic potential of QQMNTx, fibrotic area in ischemic ATM was detected by Azan staining on day 21 after treatment. The mean fibrotic area (% fibrotic area/ $\times 40$ HPF) for the QQMNTx, PBMNCTx, and control groups were 2.78 ± 0.61 , 8.41 ± 1.51 , and 11.94 ± 3.59 .

These findings indicate that QQMNTx exerted greater antifibrotic effects than did PBMNCTx (Figure 9A and 9B).

In the respective comparison among the QQMNTx, GmCD34Tx, eEPCTx, and control groups, the mean fibrotic areas (% fibrotic area/ $\times 40$ HPF) for each group were 5.89 ± 1.12 , 8.06 ± 1.05 , 11.07 ± 1.19 , and 17.04 ± 1.75 (Figure 9C and 9D). QQMNTx as well as GmCD34Tx featured superior antifibrotic effects to control and further exerted greater effects than eEPCTx.

We performed IHC of iNOS in ischemic ATM to assess inflammation. The mean iNOS-expressing areas (% iNOS-expressing area/ $\times 20$ HPF) for the QQMNTx, PBMNCTx, and control groups were 3.16 ± 0.58 , 6.26 ± 0.89 , and 21.31 ± 2.26 (Figure 10A and 10B). These findings indicate that QQMNTx inhibited inflammation more markedly than PBMNCTx.

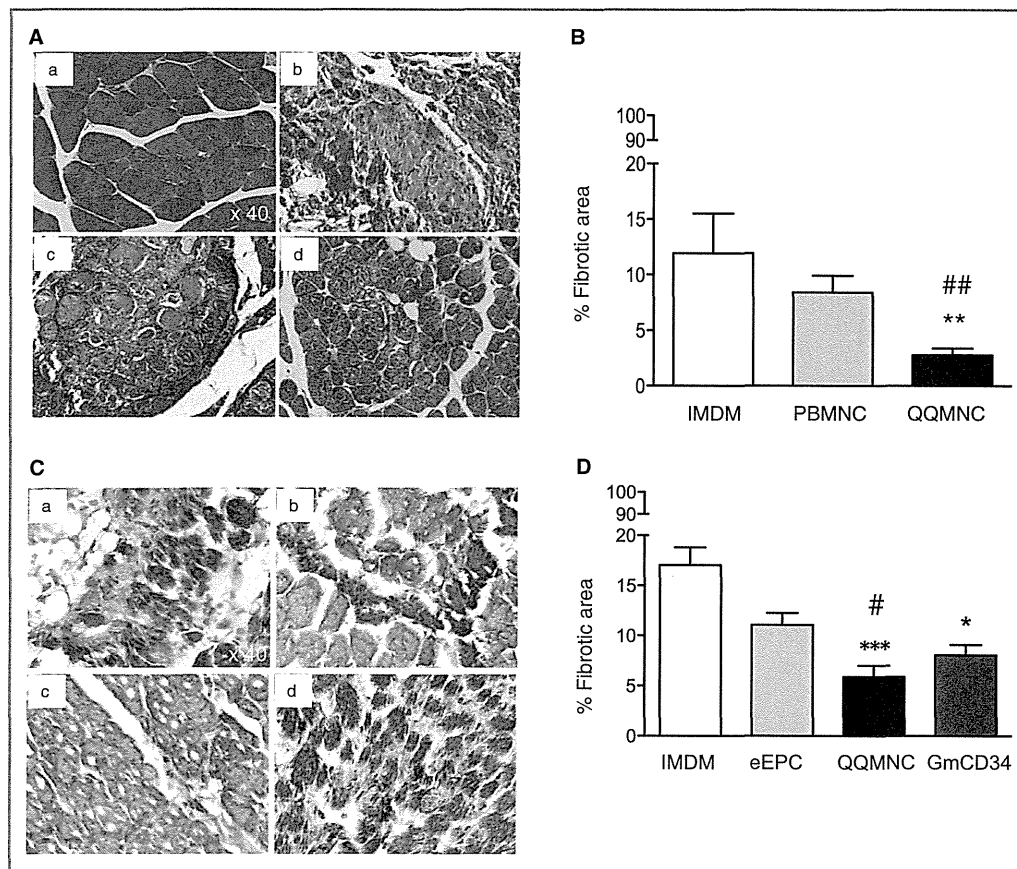


Figure 9. Histological evaluation of fibrosis in ischemic hindlimbs. A and C, Representative pictures of fibrosis in ATM assessed by Azan staining (blue) in each group. $\times 40$ HPF. (a) Contralateral hindlimb of IMDM control (b, c, and d) and ischemic hindlimbs of IMDM control, PBMNCTx, and QQMNCTx in (A). (a, b, c, and d) Ischemic hindlimbs of IMDM control, eEPCTx, QQMNCTx, and GmCD34Tx in (C). B and D, The graphs show percent (%) fibrotic area in each group. $*P < 0.05$; $**P < 0.01$; $***P < 0.001$ versus IMDM control in (B and D). $##P < 0.01$ versus PBMNCTx in (B). $\#P < 0.05$ versus eEPCTx in (D). Each column in the graph represents a mean \pm SE. $N = 6$ mice per group. ATM indicates anterior tibial muscle; eEPCTx, early endothelial progenitor cell transplantation; GmCD34, granulocyte colony-stimulating factor mobilized CD34⁺ cell; HPF, high power field; PBMNCTx, peripheral blood mononuclear cell transplantation; QQMNCTx, quality and quantity control culture of mononuclear cell transplantation.

In the respective comparison among the QQMNCTx, GmCD34Tx, eEPCTx, and control groups, the mean iNOS-expressing areas (% iNOS-expressing area/ $\times 20$ HPF) for the respective groups were 4.97 ± 0.95 , 6.07 ± 0.81 , 9.75 ± 1.09 , and 18.15 ± 1.44 (Figure 10C and 10D). In the same manner as antifibrotic aspects, QQMNCTx as well as GmCD34Tx featured superior anti-inflammation effects to control and further displayed greater effects than eEPCTx.

These findings indicate that QQMNCTx, similarly to GmCD34Tx, potentiated protective effects against inflammation and fibrosis in the ischemic hindlimb.

QQMNCTx Enhances Gene Expression for Tissue Regeneration in Ischemic Muscle

The qRT-PCR assay was implemented for murine mRNA transcripts encoding the following factors: IL-1 β (proangiogen-

ic/-inflammatory), transforming growth factor beta (TGF- β ; proangiogenic/anti-inflammatory), IGF-1 (proangiogenic/-myogenic), or MyoD1 and myogenin (promyogenic transcription).

In the comparison of the murine transcripts among the QQMNCTx, PBMNCTx, and control groups, gene expression of MyoD1, myogenin, and IGF-1 was significantly augmented by responding to QQMNCTx, but not to PBMNCTx.

Likewise, in the comparison among the QQMNCTx, GmCD34Tx, and eEPCTx groups, gene expression of MyoD1, myogenin, and IGF-1 was significantly enhanced by responding to QQMNCTx, equally to GmCD34Tx, but not to eEPCTx.

The relative ratio of each gene expression in PBMNCTx, QQMNCTx, GmCD34Tx, and eEPCTx versus that in IMDM control was as follows: 1.22 ± 0.05 , 2.58 ± 0.63 , 2.94 ± 0.61 , and 1.06 ± 0.08 in MyoD1; 1.90 ± 0.10 , 2.94 ± 0.49 , 2.69 ± 0.41 , and 0.84 ± 0.06 in myogenin; and 1.17 ± 0.11 ,

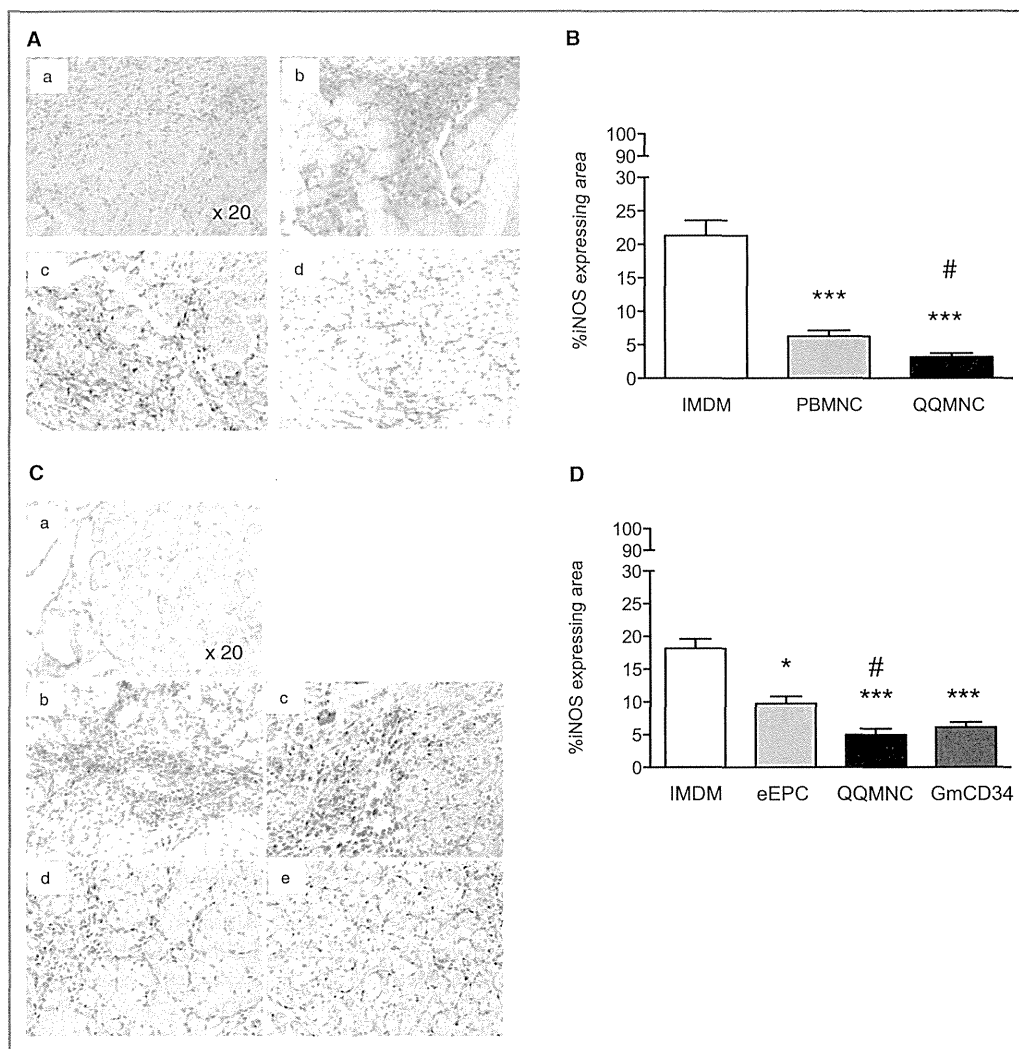


Figure 10. Histological evaluation of inflammation in ischemic hindlimbs. A and C, Representative pictures of inflammation in ATM by immunohistochemistry using anti-iNOS antibody (brown color) in each group. $\times 20$ HPF. (a) Control of rabbit polyclonal IgG, (b) IMDM control, (c) PBMNCTx, and (d) QQMNCTx in (A). (a) Control of rabbit polyclonal IgG, (b) IMDM control, (c) eEPCTx, (d) QQMNCTx, and (e) GmCD34Tx in (C). B and D, The graphs show percent (%) iNOS expressing area in each group. $*P < 0.05$; $***P < 0.001$ versus IMDM control in (B and D). $\#P < 0.05$ versus PBMNCTx in (B) or eEPCTx in (D). Each graph column represents a mean \pm SE. $N = 6$ mice per group. ATM indicates anterior tibial muscle; eEPCTx, early endothelial progenitor cell transplantation; GmCD34, granulocyte colony-stimulating factor mobilized CD34⁺ cell; HPF, high power field; iNOS, inducible nitric oxide synthase; PBMNCTx, peripheral blood mononuclear cell transplantation; QQMNCTx, quality and quantity control culture of mononuclear cell transplantation.

2.06 ± 0.40 , 2.20 ± 0.56 , and 1.00 ± 0.11 in IGF-1, respectively (Figure 11A and 11B).

The gene expression of TGF- β was fairly promoted by responding to QQMNCTx, rather than to PBMNCTx, and also enhanced equal to or higher than that in GmCD34Tx, although not in eEPCTx. The relative ratio of TGF- β gene expression in PBMNCTx, QQMNCTx, GmCD34Tx, and eEPCTx, control, was 3.14 ± 0.42 , 4.35 ± 0.60 , 3.52 ± 0.36 , and 0.52 ± 0.04 (Figure 11A and 11B).

Thus, gene expressions of the potent factors for angiogenesis, myogenesis, and anti-inflammation reacting to

QQMNCTx as well as GmCD34Tx were similarly up-regulated, when compared with those to PBMNCTx or eEPCTx.

Above all, the gene expression encoding IGF-1 to QQMNCTx was unambiguously enhanced, compared with that to the other Tx groups of PBMNCTx and eEPCTx. The findings correspond with the histological results to show the multi-functional mechanisms of QQMNCTx as superior to those of PBMNCTx or eEPCTx.

Notably, Tx of all cell sources, more or less, up-regulated gene expression of IL-1 β , a proinflammatory factor, whereas unpurified EPC Tx of QQMNCs as well as PBMNCs tended to

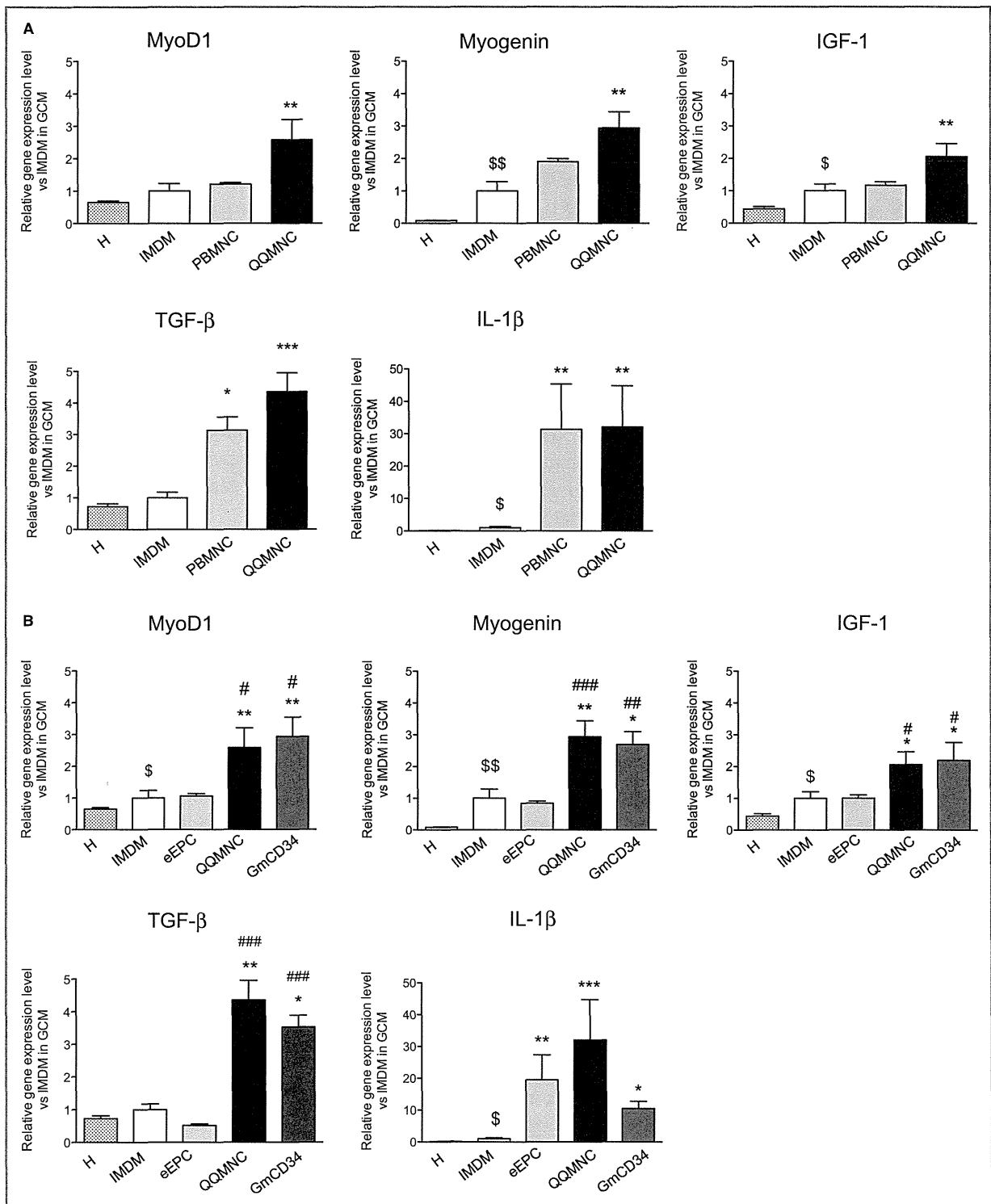


Figure 11. qRT-PCR assay of murine gene expression in ischemic hindlimbs. The graphs show the relative gene expression levels of promyogenic (MyoD1, myogenin, and IGF-1), anti-inflammation (TGF-β), and proangiogenic (IL-1β) factors. The comparison of the levels in QQMNCTx to those in IMDM control or PBMNCTx in (A) and in IMDM control, eEPCTx, and GmCD34Tx in (B). H, healthy (contralateral) hindlimb of IMDM control mice. * $P < 0.05$; ** $P < 0.01$; *** $P < 0.001$ versus IMDM control. \$ $P < 0.05$; \$\$ $P < 0.01$ versus H. # $P < 0.05$ in (A and B). ## $P < 0.01$; ### $P < 0.001$ versus eEPCTx in (B). Each graph column represents a mean \pm SE. $N = 4$ to 6 mice per group. eEPCTx indicates early endothelial progenitor cell transplantation; GCM, gastrocnemius muscle; GmCD34, granulocyte colony-stimulating factor mobilized CD34⁺ cell; IGF, insulin-like growth factor; IL, interleukin; PBMNCTx, peripheral blood mononuclear cell transplantation; QQMNCTx, quality and quantity control culture of mononuclear cell transplantation; qRT-PCR, quantitative real-time polymerase chain reaction; TGF, transforming growth factor.

produce the transcript more drastically than the purified EPC Tx of GmCD34 or eEPCs. The relative ratio of IL-1 β gene expression in QQMNC Tx, GmCD34Tx, and eEPC Tx versus that in IMDM control was 32.00 ± 12.74 , 10.47 ± 2.27 , and 19.53 ± 7.78 , respectively.

In the present experiments, PBMNC Tx, despite the fairly high expression of IL-1 β , did not exert angiogenic ability, whereas GmCD34Tx, even in the lesser expression, did so favorably. In other words, IL-1 β production in ischemic tissue responding to any cell Tx did not seemingly contribute to angiogenesis for vascular regeneration.

Discussion

Here, we developed and characterized QQMNCs (novel therapeutic cells), QQMNCs derived from PBMNCs that were subjected to QQ culture, and this QQ culture promoted expansion of EPCs and adoption of regenerative phenotypes by macrophages and T lymphocytes. The QQ culture that we used to generate QQMNCs was based on a well-established QQ culture that increases the quality and quantity of EPCs from enriched EPC populations, such as CD34⁺ and CD133⁺ cells; this established QQ culture was used to generate therapeutic stem cells for CV regeneration in rat infarcted myocardia.²³

We found here that the vasculogenic signaling condition of this QQ culture potentiated the vascular regeneration ability of naïve PBMNCs to produce QQMNCs. QQMNCs were superior to PBMNCs, and equal to or greater than GmCD34 cells, in terms of regeneration abilities, including vascular regeneration (angiogenesis, arteriogenesis, and vasculogenesis), myogenesis, anti-inflammation, and antifibrosis.

EPC Expansion and Differentiation in QQMNCs

EPC-CFA of QQMNCs demonstrated intensive expansion potential of colony-forming EPCs, especially dEPCs (Figure 1D). The concept of colony-forming EPCs was recently introduced.^{12,38} pEPCs in small-sized EPC colonies showed a higher rate of proliferation and a higher percentage of cells in S-phase, when compared to dEPCs in large-sized EPC colonies. In contrast, dEPCs had a significantly higher capacity for vasculogenic activity than did pEPCs; similarly, dEPCs also had a greater overall potential for cell adhesion and formation of tube-like structures *in vitro*; importantly, dEPCs had a greater capacity than pEPCs to support *de novo* blood vessel formation *in vivo* after transplantation into ischemic models.

Therefore, pEPCs are defined as very immature, highly proliferative EPCs; in contrast, dEPCs are believed to derive from pEPCs and represent cells prone to differentiation and promotion of vasculogenesis. These dEPCs are proven to play a key role in vasculogenesis, and to be suitable for vascular

regeneration therapy. In this regard, QQ culture promoted significant expansion and commitment of colony-forming EPCs with vasculogenic potential.

To confirm colony-forming EPC expansion in QQ culture of naïve PBMNCs, we evaluated EPC colony-forming activity before and after QQ culture (Figure 1E). Total EPC-CFU count in QQMNC samples was correlated with that in PBMNC samples. For example, pEPC-CFU count in PBMNC samples correlated with dEPC-CFU count and with total EPC-CFU count in QQMNC samples, but not with pEPC-CFU count in QQMNC samples. The dEPC-CFU count in PBMNC samples did not correlate to any EPC-CFU count in QQMNC samples. These data indicate that signals in QQ culture probably induced concurrent expansion and differentiation of pEPC-CFCs, resulting in an increase in the dEPC-CFC population instead of the pEPC-CFC population. Consequently, the enhanced vasculogenic potential of post QQ culture-treated cells, compared with the precursor PBMNCs, explained the preferential vascular regeneration.

Cell Populations in QQ Cultures

The cell numbers of QQMNCs were, on average, approximately half of those in the respective PBMNCs. The cellular density of PBMNCs per blood volume is inversely correlated with the ratio of cellular density per well between PBMNCs and QQMNCs. Therefore, the QQMNC numbers are rather dependent on the original blood volume per se (Figure 1B).

From the view of cell populations, the decrease in total cell count is mainly derived from significant reduction of B lymphocytes (CD19⁺), NK cells (CD16⁺ and CD56⁺), cytotoxic T cells (CD8⁺), and proinflammatory monocytes and macrophages (CD14⁺ and CCR2⁺). In contrast, populations of progenitor cells (CD34⁺ and CD133⁺) and of anti-inflammatory monocytes and macrophages (CD206⁺) expanded greatly, but populations of endothelial cells (CD105⁺ and CD146⁺) and helper T cells (CD4⁺) expanded only moderately.

The increase in CD34⁺ or CD133⁺ cell populations indicates the expanded population of immature EPCs. The increase in CD105⁺ or CD146⁺ cell populations was also indicative of EPC expansion and differentiation; notably, differentiating EPCs express these markers.^{39,40}

The extent of the increase in CD206⁺ cells and of the decrease in CCR2⁺ cells indicates the conversion of the monocyte/macrophage phenotype from M1 to M2 type. Monocytes/macrophages differentiate toward a proinflammatory, classically activated M1 state or toward an anti-inflammatory, alternatively activated M2 state according to different environments and stimuli. M1 macrophages are induced by proinflammatory cytokines and microbial products, such as INF- γ , tumor necrosis factor alpha (TNF- α), and lipopolysaccharide; these macrophages are mainly associated with pathologic inflammations. M2 macrophages are induced